environmental microbiology

Environmental Microbiology (2016) **18**(9), 3073–3091 doi:10.1111/1462-2920.13283

Candidatus Desulfofervidus auxilii, a hydrogenotrophic sulfate-reducing bacterium involved in the thermophilic anaerobic oxidation of methane

Viola Krukenberg,[1]* Katie Harding,[1†] Michael Richter,[1] Frank Oliver Glöckner,[1,2] Harald R. Gruber-Vodicka,[1] Birgit Adam,[1‡] Jasmine S. Berg,[1] Katrin Knittel,[1] Halina E. Tegetmeyer,[3,4] Antje Boetius[1,3,5] and Gunter Wegener[1,5]

[1]*Max Planck Institute for Marine Microbiology, Bremen, Germany.*

[2]*Jacobs University Bremen gGmbH, Bremen, Germany.*

[3]*Alfred Wegener Institute, Helmholtz Center for Polar and Marine Research, Bremerhaven, Germany.*

[4]*Center for Biotechnology, Bielefeld University, Bielefeld, Germany.*

[5]*MARUM, Center for Marine Environmental Sciences, University Bremen, Bremen, Germany.*

Summary

The anaerobic oxidation of methane (AOM) is mediated by consortia of anaerobic methane-oxidizing archaea (ANME) and their specific partner bacteria. In thermophilic AOM consortia enriched from Guaymas Basin, members of the ANME-1 clade are associated with bacteria of the HotSeep-1 cluster, which likely perform direct electron exchange via nanowires. The partner bacterium was enriched with hydrogen as sole electron donor and sulfate as electron acceptor. Based on phylogenetic, genomic and metabolic characteristics we propose to name this chemolithoautotrophic sulfate reducer *Candidatus* Desulfofervidus auxilii. *Ca.* D. auxilii grows on hydrogen at temperatures between 50°C and 70°C with an activity optimum at 60°C and doubling time of 4–6 days. Its genome draft encodes for canonical sulfate reduction, periplasmic and soluble hydrogenases and autotrophic carbon fixation via the reductive tricarboxylic acid cycle. The presence of genes for pili formation and cytochromes, and their similarity to genes of *Geobacter* spp., indicate a potential for syntrophic growth via direct interspecies electron transfer when the organism grows in consortia with ANME. This first ANME-free enrichment of an AOM partner bacterium and its characterization opens the perspective for a deeper understanding of syntrophy in anaerobic methane oxidation.

Received 21 October, 2015; revised 23 February, 2016; accepted 24 February, 2016. *For correspondence. E-mail vkrukenb@mpi-bremen.de; Tel. 0049 421 2028 984; Fax 0049 421 2028 870. Present addresses: †Department of Ocean Sciences, University of California, Santa Cruz, CA, USA. ‡Department of Communications, Max-Planck-Gesellschaft zur Förderung der Wissenschaften e.V., München, Germany.

Introduction

The microbially mediated anaerobic oxidation of methane (AOM) is a key process in anoxic methane-rich marine habitats, controlling methane efflux from the seabed (Boetius and Wenzhöfer, 2013). Marine AOM is performed by consortia of anaerobic methane-oxidizing archaea (ANME) and partner bacteria coupling the oxidation of methane to the reduction of sulfate in a syntrophic process (Boetius *et al.*, 2000; Orphan *et al.*, 2001b). The oxidation of methane is mediated by the archaea, involving the reversal of the methanogenesis pathway (Hoehler *et al.*, 1994; Hallam *et al.*, 2004). Previous studies have assigned canonical sulfate reduction to the consortial partner bacteria (Boetius *et al.*, 2000; Milucka *et al.*, 2013). The mode of interspecies transfer of electrons from the ANME to the sulfate-reducing partner bacteria remains uncertain. Exchange of metabolic intermediates, hydrogen or direct interspecies electron transfer have been discussed (Hoehler *et al.*, 1994; Widdel *et al.*, 2007; Moran *et al.*, 2008; McGlynn *et al.*, 2015; Wegener *et al.*, 2015). Alternatively, it was suggested that the archaea could carry out partial sulfate reduction, with the bacterial partner disproportionating zero-valent sulfur species (Milucka *et al.*, 2012). AOM is mediated by members of three different phylogenetic clades [ANME-1, ANME-2 and ANME-3; (Knittel and Boetius, 2009)] which comprise a substantial diversity of subgroups (Ruff *et al.*, 2015). Although the consortia formed by the different ANME are highly specific associations with only one type of partner bacterium, there is a considerable diversity of *Deltaproteobacteria* that can form AOM consortia. The Seep-SRB-1 cluster (*Desulfosarcina*/*Desulfococcus*) prevails in most natural and laboratory psychro- and mesophilic enrichments

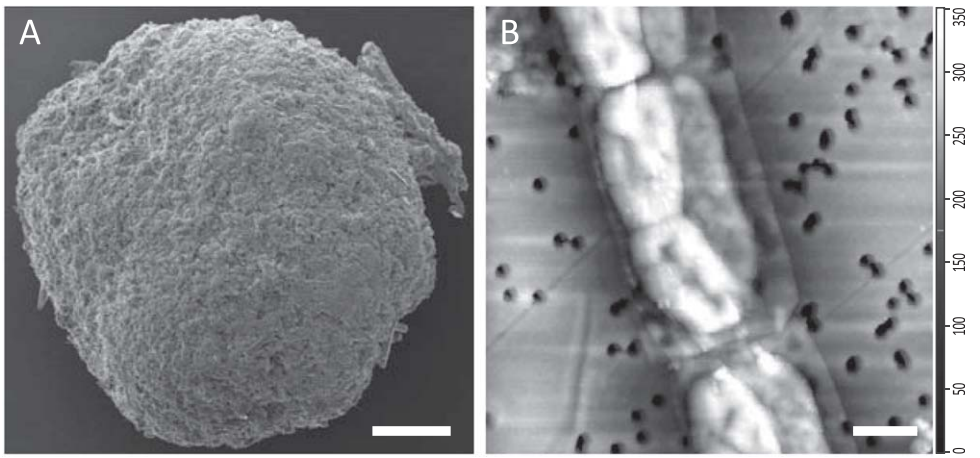

Fig. 1. Microbial consortia from thermophilic AOM enrichments. A. SEM image of a spherical TAOM aggregate, scale 100 μm. B. AFM image of a component of a TAOM filament showing close proximity of archaeal (left) and bacterial (right) cells in a common envelope, visualized on a 0.2 μm pore-size filter, scale 1 μm, grey gradient bar indicates object height in nm.

dominated by ANME-2 (Boetius *et al*., 2000; Orphan, *et al*., 2001a; Michaelis *et al*., 2002; Knittel *et al*., 2003). The Seep-SRB-2 cluster is frequently observed as partner of psychro- and mesophilic ANME-1 and -2 (Kleindienst *et al*., 2012; Wegener *et al*., 2016) and *Desulfobulbus*-relatives as partner of ANME-3 (Niemann *et al*., 2006). None of the psychro- to mesophilic ANME or their partner bacteria have yet been obtained as pure culture hence some of these organisms might be obligate syntrophs.

Here, we studied the bacterial partner in thermophilic AOM (growth range 50°C–65°C), HotSeep-1, recently enriched from the methane-rich hydrothermal system of the Guaymas Basin, Gulf of California (Holler *et al*., 2011). In thermophilic AOM enrichments HotSeep-1 bacteria associate with ANME-1 archaea to form filamentous or densely packed spherical consortia. So far, DNA sequences similar to those of this bacterial partner have only been reported from hydrothermal vent systems (Teske *et al*., 2002; Biddle *et al*., 2011; Dowell *et al*., 2016), and thermophilic short-chain hydrocarbon-degrading enrichments originating from the Guaymas Basin (butane-degrading) and from Middle Valley, Juan de Fuca Ridge (ethane-, propane- and butane-degrading) (Kniemeyer *et al*., 2007; Adams *et al*., 2013). In thermophilic AOM, HotSeep-1 retrieves reducing equivalents from its ANME partner through the oxidation of methane (Holler *et al*., 2011) likely via direct interspecies electron transfer (Wegener *et al*., 2015).

We highlight here the metabolic and genomic features of a representative of the HotSeep-1 cluster, proposed as *Candidatus* Desulfofervidus auxilii, with the focus on its potential role as syntrophic partner in hydrocarbon degradation.

Results and discussion

Enrichment and cultivation of HotSeep-1

During thermophilic anaerobic oxidation of methane (TAOM), HotSeep-1 formed dense cell aggregates with ANME-1 archaea in the form of filaments or large spherical aggregates (Fig. 1). In filaments, HotSeep-1 and ANME-1 cells associated in close proximity and often 1:1 stoichiometry within a sheath-like structure (Holler *et al*., 2011; Fig. 1B). Spherical aggregates reaching sizes of 0.5 mm contained well-mixed, approximately equal portions of HotSeep-1 and ANME-1 cells and were the dominant consortia growth type in long-term, sediment-free TAOM enrichments (>2 years of enrichment by continuous dilution) (Fig. 1A). When the energy supply to the TAOM enrichment was switched from methane to hydrogen, the enrichment responded with a fivefold increase of the sulfide production rate as calculated from the first 9 days (Fig. 2A). Other substrates (a variety of organic compounds including acetate, formate, alcohols, benzoate, dicarboxylic acids, pyruvate, methyl sulfide and carbon monoxide) did not lead to sulfide production (see Wegener *et al*., 2015). Serial dilution to extinction cultivation of this enrichment at 60°C with sulfate and hydrogen as the energy source, and inorganic carbon as the sole carbon source, resulted in separation of HotSeep-1 cells from the ANME partner in initial dilutions of up to $1{:}10^6$. Continuous dilution yielded an enrichment of >95% HotSeep-1 cells (Fig. 2B–D). A persistent archaeal contaminant, identified as *Archaeoglobus* sp. by 16S rRNA gene sequencing, accounted for around 5% of all cells during the exponential growth phase (Supplementary Fig. S1). Taxonomic classification of metagenomic 16S rRNA gene fragments (approximately 2000 reads) obtained from the enrichment estimated HotSeep-1 to *Archaeoglobus* sp. 16S rRNA genes in a ratio >100:1. Accordingly, the nearly full length 16S rRNA gene sequences assembled from the metagenome, which related to HotSeep-1 and *Archaeoglobus fulgidus* showed coverages of 108x and 3x respectively. ANME-1 was not detected in the hydrogenotrophic HotSeep-1 enrichment. Based on phylogenetic, genomic and metabolic data we propose that the enriched HotSeep-1 represents a novel species, *Candidatus* Desulfofervidus auxilii, referring in denotation to the bacterium's sulfate-reducing metabolism in thermophilic syntrophic consortia.

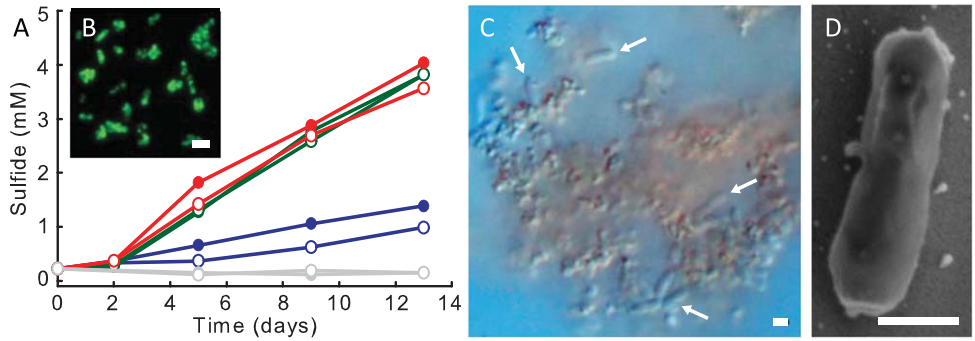

Fig. 2. Effect of hydrogen on TAOM enrichment (A) and visualization of *Ca*. D. auxilii cells (B-D).
A. Sulfide production in thermophilic AOM consortia enrichment supplied with methane (blue), methane plus hydrogen (green) or hydrogen (red), and without energy source (grey) in replicate incubations per condition (filled and open circles).
B. *Ca*. D. auxilii cells in a highly enriched culture on hydrogen; cells were visualized with the specific CARD-FISH probe HotSeep-1_1465, scale 2 μm.
C. Differential interference contrast micrograph of *Ca*. D. auxilii cells (marked by arrow) aggregating around inorganic precipitates (brownish colour), scale 1 μm. D. Scanning electron microscopy image of a *Ca*. D. auxilii cell grown on hydrogen, scale 500 nm.

Physiological characterization of Ca. D. auxilii

Hydrogen-dependent sulfate-reducing activity of *Ca*. D. auxilii cultures was observed at temperatures between 50°C and 70°C. Sulfate reduction rates were highest at 60°C (Supplementary Fig. S2). The cell specific sulfate reduction rate at 60°C was 46 fmol sulfate reduced per day per cell (Supplementary Fig. S1). No activity was observed below 50°C and above 70°C, matching the temperature optimum in consortial growth with ANME-1 (Holler *et al.*, 2011). Freshly inoculated *Ca*. D. auxilii cultures showed a relatively long lag phase of approximately 12 days followed by an exponential increase of sulfate-reducing activity, carbon fixation and cell numbers until sulfate was depleted (after about 32–35 days) (Supplementary Fig. S1). *Ca*. D. auxilii tolerates high sulfide concentrations of up to 25 mM (Supplementary Fig. S1), which is an advantage in its highly sulfidic natural habitat in subsurface sediments of methane-rich hydrothermal

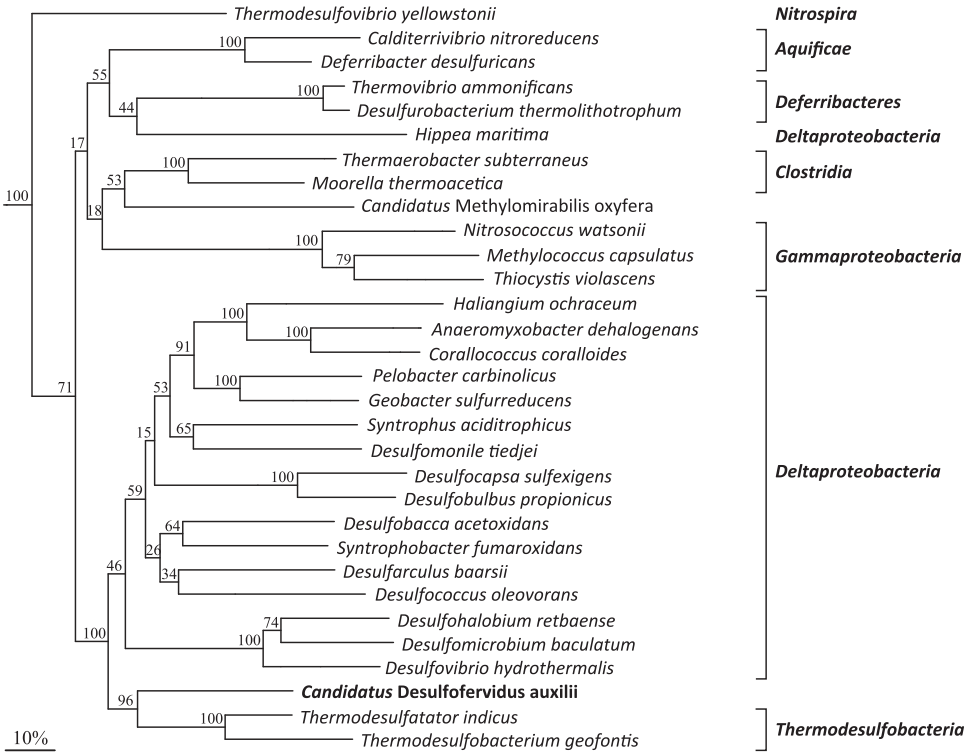

Fig. 3. Phylogenetic affiliation of *Ca*. D. auxilii reconstructed from the concatenated protein alignment of 19 universal single copy marker genes (Wu and Scott, 2012). The phylogenetic tree was calculated using the maximum likelihood algorithm (RAxML). For clarity only a subset of the tree is depicted. Values at nodes indicate branch support calculated from 100 replicates. The 16S rRNA gene based phylogenetic classification is indicated to the right and is not fully congruent with the clustering observed in the depicted single copy gene tree. *Ca*. D. auxilii branches off at the root of the *Thermodesulfobacteria*, which form a sister clade to the *Deltaproteobacteria*.

vents (Jørgensen *et al*., 1990; Vigneron *et al*., 2014). The calculated doubling time of 4–6 days is slow compared to other hydrogenotrophic sulfate reducers [doubling time of 12–24 h (Brysch *et al*., 1987; Alazard *et al*., 2003; Audiffrin *et al*., 2003; Rabus *et al*., 2006)]. However, compared with the inherently slow growth as partner bacterium in thermophilic AOM (doubling time approx. 50 days as estimated from the increase in sulfide production), growth dynamics were 12 times faster in single culture on hydrogen. Organic compounds (including acetate, formate, alcohols, benzoate, dicarboxylic acids, pyruvate, methyl sulfide and carbon monoxide) were neither used as energy source for sulfate reduction nor did they support growth of *Ca*. D. auxilii cells (Supplementary Fig. S3), which is in agreement with the absence of sulfide production in TAOM enrichments supplemented with organic compounds other than methane (see above). Notably, no sulfate-reducing activity of *Ca*. D. auxilii was observed on methane and short-chain hydrocarbons (propane, butane), which contrasts earlier reports of HotSeep-1 dominated short-chain hydrocarbon-degrading enrichments (Adams *et al*., 2013) (Supplementary Figs. S3 and S4). Further, tested organic compounds did not substantially stimulate hydrogenotrophic sulfate-reducing activity or growth of *Ca*. D. auxilii suggesting that *Ca*. D. auxilii grows autotrophically (Supplementary Fig. S5). Some organic compounds even inhibited growth (methanol, lactate, propionate, yeast extract), an effect previously observed for thermophilic hydrogenotrophs (Kawasumi *et al*., 1980; Kristjansson *et al*., 1985). Autotrophic growth of *Ca*. D. auxilii is in line with earlier studies on other sulfate-reducing AOM partner bacteria also showing carbon dioxide fixation (Wegener *et al*., 2008; Kellermann *et al*., 2012). Autotrophic carbon fixation by *Ca*. D. auxilii accounts for on average 0.03–0.04 mol carbon dioxide fixed per mol sulfate reduced (Supplementary Fig. S6) with a carbon fixation rate of 1.3 fmol per day per cell. This corresponds to the use of only 1.5% of the reducing equivalents derived from hydrogen oxidation for carbon fixation. This carbon fixation capacity is much lower than in other studied hydrogenotrophic sulfate reducers (Brandis and Thauer, 1981; Cypionka and Pfennig, 1986), which explains the comparatively low growth rates and limited cell densities of the *Ca*. D. auxilii culture. It compares well with the carbon fixation capacity in TAOM of 2%, when determined as reducing equivalents derived from methane oxidation (Wegener *et al*., 2015). Furthermore, neither reduction nor disproportionation of alternative sulfur sources (i.e. sulfite, thiosulfate and elemental sulfur) sustained growth of *Ca*. D. auxilii (Supplementary Fig. S7), indicating that *Ca*. D. auxilii is an obligate sulfate reducer.

Phylogenetic position of Ca. D. auxilii

Ca. D. auxilii is the first cultured representative of a 16S rRNA gene sequence cluster (>97.5% similarity) which to date comprises almost full length sequences (>1400 bp) obtained from Guaymas Basin environmental samples (Teske *et al*., 2002; Dowell *et al*., 2016) and methane- and butane-degrading enrichments (Kniemeyer *et al*., 2007; Holler *et al*., 2011; Kellermann *et al*., 2012; Wegener *et al*., 2015), and additionally assigned partial sequences retrieved from Middle Valley hydrocarbon-degrading enrichments (NCBI SRA066151) (Adams *et al*., 2013). The first sequences of this cluster were identified by Teske *et al*. (2002) as 'Guaymas-specific sequence cluster'. Later, when Holler *et al*. (2011) assigned similar sequences to the bacterial partner in thermophilic AOM the cluster was denoted 'HotSeep-1'. The genomic 16S rRNA gene obtained from the hydrogenotrophically grown *Ca*. D. auxilii is identical or highly similar to sequences of the HotSeep-1 cluster (see Supplementary Table S1). Previous phylogenetic classifications of this cluster in the 16S rRNA gene based phylogenetic tree are discordant and have described it as a member of the *Deltaproteobacteria* with *Desulfurella* and *Hippea* as distant relatives (Holler *et al*., 2011) or as an independent lineage (Teske *et al*., 2002; Dowell *et al*., 2016). Our 16S rRNA gene phylogenetic analysis confirmed a deep-branching position of this cluster (Supplementary Fig. S8) (Teske *et al*., 2002; Holler *et al*., 2011; Dowell *et al*., 2016) and showed that its affiliation within the bacterial phylogenetic tree varied considerably depending on the method and the set of reference sequences used for tree calculation, which indicates insufficient phylogenetic context for this cluster on the 16S rRNA gene level. To further resolve the phylogenetic classification of *Ca*. D. auxilii we reconstructed the phylogeny based on different marker genes and gene sets. A phylogenomic approach using a set of 19 single copy housekeeping genes (detected in all here analysed genomes; see Supplementary Discussion and Supplementary Table S2) revealed a sister relationship of *Ca*. D. auxilii to members of the *Thermodesulfobacteria*, namely *Thermodesulfatator indicus* and *Thermodesulfobacterium geofontis*, and an affiliation of this cluster as sister clade to the *Deltaproteobacteria* (Fig. 3; see also Supplementary Discussion). An affiliation with the *Deltaproteobacteria* was supported by the 23S rRNA gene based phylogeny, which placed *Ca*. D. auxilii within the *Deltaproteobacteria* with *Desulfobacca acetoxidans*, *Geobacter* spp. and *Syntrophobacter fumaroxidans* as its closest relatives (Supplementary Fig. S9). The latter two are known to often grow as syntrophs (McInerney *et al*., 2009). We also used the dissimilatory sulfite reductase (Dsr) gene, encoding a key enzyme of sulfate reduction and used as a functional marker gene of sulfate reducers, for phylogenetic analysis (Klein *et al*., 2001; Müller *et al*., 2014). The amino acid sequence of the Dsr subunit A (DsrA) of *Ca*. D. auxilii affiliated with DsrA sequences from *Desulfatiglans anilini* (formerly *Desulfobacterium anilini*), *Moorella thermoacetica* and *Desulfotomaculum* spp. (Supplementary Fig. S10; see also Supplementary

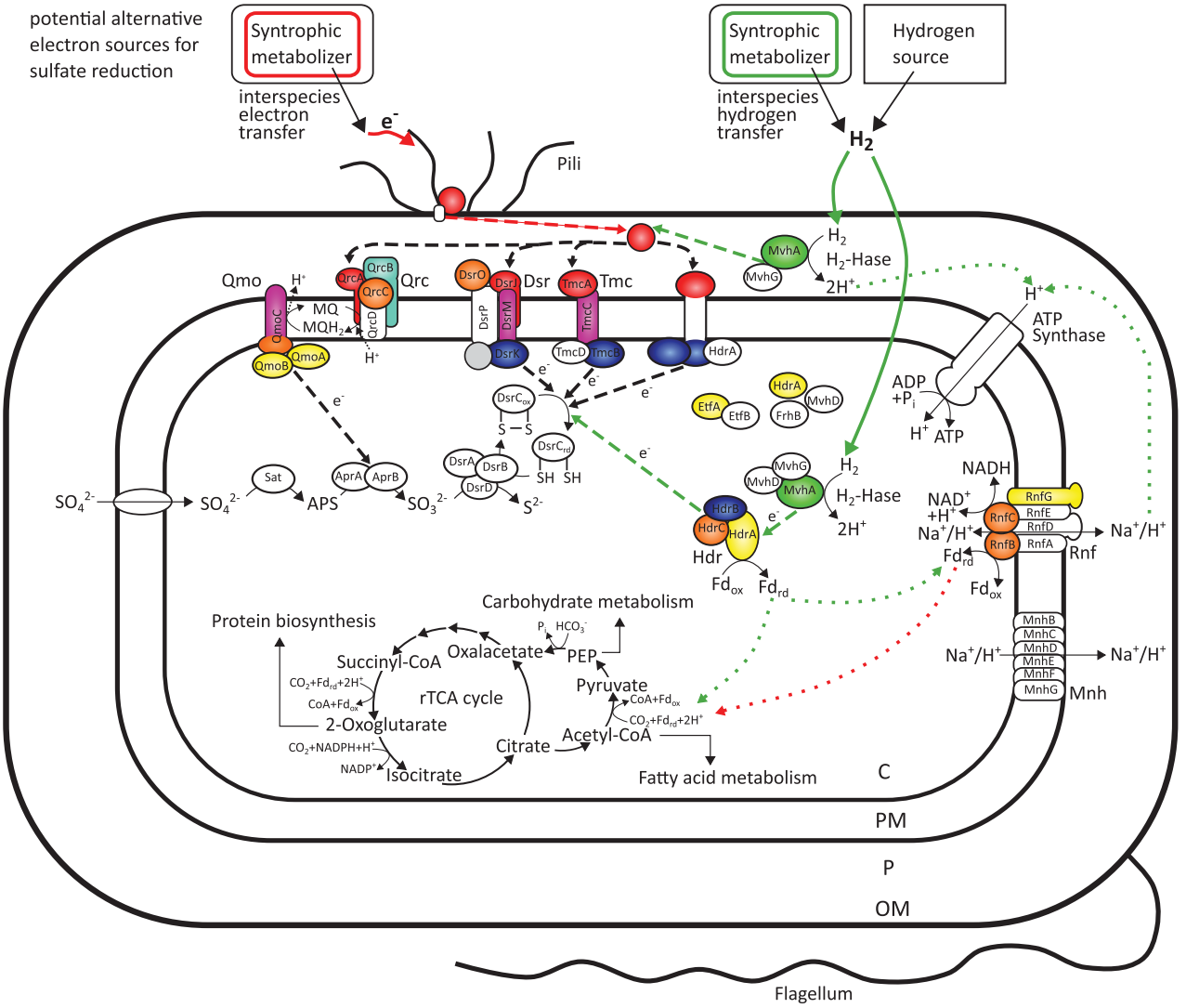

Fig. 4. Scheme of energy metabolism and autotrophic carbon fixation in *Ca.* D. auxilii reconstructed from its draft genome. Depicted are the proposed reducing equivalent entry points during the possible alternative growth strategies of *Ca.* D. auxilii via hydrogen, green arrows (either supplied hydrogen or syntrophic interspecies hydrogen transfer) or via DIET, red arrow. Colour coding: red for c-type cytochrome, purple for b-type cytochrome, orange for FeS proteins, turquoise for molybdopterin family proteins, dark blue for CCG proteins, yellow for flavoproteins, green for hydrogenase (catalytic subunit), white means not assigned and grey indicates protein may represent an additional subunit. Protein complex structure is adapted from previous models (Pereira *et al.*, 2011). Dashed lines represent potential electron flow pathways. Dotted lines represent proton flow pathways or possible ferredoxin linkage. Black line colour: path predicted to exist during growth with hydrogen and DIET; red line colour: path predicted to only exist during growth via DIET; green line colour: path predicted to exist only during growth on hydrogen. Rnf complex is depicted as working in both directions. C, Cytoplasm; PM, Periplasmic membrane; P, Periplasm; OM, Outer membrane.

Discussion), with highest amino acid sequence similarity (75%) to *D. anilini* (*Deltaproteobacteria*).

In summary, our phylogenetic analyses of multiple genes/gene sets and whole genome comparison (see Supplementary Discussion and Supplementary Table S3 and S4) as well as physiologic characteristics (see Table 1) revealed similarity (phylogenetic and metabolic) of *Ca.* D. auxilii to members of the *Deltaproteobacteria* and *Thermodesulfobacteria*, although a classification into either of the two groups currently is not well supported on the 16S rRNA gene level. However, a database comparison of the genomic 16S rRNA gene of *Ca.* D. auxilii showed among the top 10 hits (84%–86% identity) to cultured organisms members of *Deltaproteobacteria* and *Thermodesulfobacteria*, with the best scoring hit (86% similarity) to *Thermodesulforhabdus norvegicus* (*Deltaproteobacteria*) (Supplementary Table S5). According to recent taxonomic thresholds defined in Yarza *et al.*

Table 1. Morphological and physiological characteristics of *Ca*. D. auxilii.

Characteristic	*Ca*. D. auxilii
Cell morphology	rod
Cell size (μm)	1.5–2.0 x 0.5
Doubling time (days)	4–6
Temperature range (°C)	50–70
Activity optimum (°C)	60
Carbon source	CO_2
Electron acceptors	
Sulfate	+
Sulfite	−
Thiosulfate	−
Sulfur[a]	−
Electron donors	
H_2	+
Formate	−
Acetate	−
Hydrocarbons[b]	−
other organic compounds[c]	−
Disproportionation	
Sulfite	−
Thiosulfate	−
Sulfur[a]	−
Syntrophic growth[d]	+

a. Sulfur was provided in form of either S° powder or as colloidal S°.
b. Methane, propane and butane were tested.
c. Other organic electron donors tested: pyruvate, lactate, propionate, benzoate, succinate, fumarate, malate, methanol, ethanol, glucose, fructose, peptone, yeast extract, carbon monoxide, methyl sulfide.
d. Determined as consortial growth in AOM enrichments with methane as substrate.

(2014), a 16S rRNA gene sequence similarity of ≤86.2% suggests a membership in different families. Hence, we propose that *Ca*. D. auxilii and related sequences in the HotSeep-1 cluster represent a novel family, *Candidatus* Desulfofervidaceae. A clear classification on higher taxonomic level (above family) awaits clarification by isolating and describing further members of this novel deep-branching lineage.

General genome features

The here described draft genome of *Ca*. D. auxilii has a size of 2.55 Mbp and a GC content of 37%. The obtained sequencing data provided an estimated 430 fold coverage of the genome. In total, 2528 open reading frames (ORFs) were identified of which about 66% (1658 ORFs) could be assigned to COG (clusters of orthologous genes) categories (see Supplementary Table S6 for an overview of observed COG categories). The genome contains one 16S-23S-5S rRNA operon and 47 tRNAs. Genome completeness was almost reached, based on estimations by (i) the checkM software (Parks *et al*., 2015) using 340 marker genes (97% completeness with 4% contamination and without detected strain heterogeneity) and (ii) the AMPHORA2 package with 31 bacterial marker genes (all detected, *dna*G duplicated) (Wu and Scott, 2012), and (iii) based on the detection of tRNAs for all amino acids. The general genome features are summarized in Table 2. The draft genome of *Ca*. D. auxilii's is comparable in size and GC content to genomes of other sulfate- and sulfur-reducing bacteria retrieved from hydrothermal habitats such as *Thermodesulfatator indicus* (2.5 Mbp, GC content 40%), *Thermodesulfobacterium geofontis* (1.3 Mbp, GC content 30%), and *Hippea maritima* (1.7 Mbp, GC content 37%) (Anderson *et al*., 2004; Huntemann *et al*., 2011; Elkins *et al*., 2013). In the course of evolution genome reduction might occur as a result of adaptation to specific environmental niches, thus *Ca*. D. auxilii's limited metabolic versatility is presumably reflected in its small genome size.

Table 2. Draft genome sequence information.

Feature	Value
Scaffolds	1
Genome size (bp)	2 540 211
coding DNA sequence (bp)	2 286 941
coding DNA sequence (%)	>90
N (%)	<1
GC content (%)	37
ORFs	2528
genes assigned to COGs	1658
rRNAs (5S, 16S, 23S)	3
tRNAs	47
tRNA completeness (%)[a]	100
Single copy gene completeness (%)[b]	97–100

a. Estimate of completeness based on identification of at least one tRNA for each amino acid; tRNAscan-SE v.1.21 Lowe and Eddy (1997).
b. Estimate of completeness based on single copy gene analysis using AMPHOR2 Wu and Scott (2012) and checkM Parks *et al*. (2015) pipeline (see experimental procedures, and results and discussion).

Genomic basis for hydrogenotrophic growth of Ca. D. auxilii

Ca. D. auxilii's draft genome encodes a complete set of proteins required for hydrogen-dependent sulfate-reduction (see Fig. 4 for a graphic representation). It includes a soluble (HS1_002313-HS1_002314) and a periplasmic (HS1_000162-HS1_000163) [NiFe] hydrogenase, and proteins required for its maturation and expression (HS1_000157-HS1_000161, HS1_000149-HS1_000151). The predicted non-membrane bound periplasmic hydrogenase is proposed to transfer electrons from hydrogen oxidation to periplasmic c-type cytochromes (Matias *et al*., 2005). The identified soluble methyl-viologen-reducing

[NiFe] hydrogenase (MvhA) may form a cytoplasmic complex with heterodisulfide reductase subunits (HS1_001272-HS1_0001274) as previously suggested (Thauer *et al.*, 2008). This MvhADG/HdrABC complex may couple hydrogen oxidation to the endergonic reduction of the low-potential redox-carrier ferredoxin and the exergonic reduction of a heterodisulfide bond in a flavin-based electron bifurcation mechanism (Buckel and Thauer, 2013).

As a terminal electron sink, *Ca*. D. auxilii has a complete dissimilatory sulfate reduction pathway. It is located in the cytoplasm and consists of sulfate adenylyltransferase (Sat, HS1_002311), adenosine phosphosulfate reductase (AprAB, HS1_000253-HS1_000254) and a dissimilatory sulfite reductase complex (DsrABCD, HS1_002180-HS1_002182, HS1_000090). Electrons derived through the periplasmic oxidation of molecular hydrogen are proposed to reduce the periplasmic cytochrome pool and enter the sulfate reduction pathway via cytochrome- and menaquinone-interacting membrane-bound electron transfer complexes, several of which are known from sulfate-reducing bacteria and archaea (Pereira *et al.*, 2011). The quinone reductase complex (QrcABCD, HS1_000675-HS1_000678) was proposed to reduce the membrane menaquinone pool via electrons from periplasmic cytochromes (Venceslau *et al.*, 2010). The menaquinone-interacting oxidoreductase complex (QmoABC, HS1_002183-HS1_002185) then delivers electrons from the reduced menaquinone pool to the adenosine phosphosulfate reductase complex (Pires *et al.*, 2003; Ramos *et al.*, 2012; Grein *et al.*, 2013). The TmcABCD complex (HS1_001244-HS1_001247) and HmeABCDE (DsrMKJOP) complex (HS1_002291-HS1_002295) were suggested to directly deliver electrons from the periplasmic cytochrome pool to the cytoplasmic DsrAB complex through a reduction of the disulfide bond in DsrC via heterodisulfide reductases (Venceslau *et al.*, 2014). Electrons derived through cytoplasmic hydrogen oxidation by MvhADG/HdrABC (HS1_002313-HS1_002314/HS1_001272-HS1_0001274) possibly enter the dissimilatory sulfate reduction pathway also at the level of DsrAB via reduction of DsrC by HdrB (Pereira *et al.*, 2011; Grein *et al.*, 2013).

Energy conservation during hydrogenotrophic growth of *Ca*. D. auxilii could occur via electron transport phosphorylation utilizing the electrochemical gradient created by periplasmic hydrogen oxidation for synthesis of adenosine triphosphate (ATP) via an ATP synthase (F-type ATPase, HS1_001679-HS1_001682, HS1_001898-HS1_001904). Alternatively, *Ca*. D. auxilii may utilize a membrane-associated ion-translocating complex (Rnf complex, HS1_001621-HS1_001626) (Buckel and Thauer, 2013) which was suggested to couple the exergonic re-oxidation of reduced ferredoxin with NAD^+ to the translocation of protons (Na^+ or H^+) across the membrane, creating an electrochemical gradient for ATP synthesis (Biegel and Müller, 2010). Thus *Ca*. D. auxilii potentially conserves energy via two mechanisms: electron transport phosphorylation and electron bifurcation. However, ferredoxin is a central electron carrier and reduced ferredoxin is crucial for autotrophic carbon fixation in anaerobes. *Ca*. D. auxilii may generate reduced ferredoxin from hydrogen through cytoplasmic electron bifurcation at the MvhADG/HdrABC complex as suggested before for other sulfate reducers (Thauer *et al.*, 2008; Buckel and Thauer, 2013). Another possibility would be a reverse-functioning Rnf complex to generate additional reduced ferredoxin (e.g. for carbon fixation) with NADH (endergonic) utilizing energy conserved in the proton gradient (Schmehl *et al.*, 1993; McInerney *et al.*, 2007).

As generally observed in genomes of sulfate reducers (Strittmatter *et al.*, 2009; Pereira *et al.*, 2011) genes encoding putative heterodisulfide reductase (Hdr) subunits were also identified in the *Ca*. D. auxilii draft genome (16 putative Hdr-encoding genes). Besides the Hdr-containing membrane-bound electron transfer complexes Tmc, Dsr and Qmo an additional gene cluster was identified that potentially encodes another membrane-bound complex with Hdr-related subunits and proteins involved in electron transfer reactions (see Supplementary Fig. S11A). The predicted integral membrane protein encoded by HS1_002398 contains protein domains similar to HdrF of *Desulfobacterium autotrophicum* HMR2 (Strittmatter *et al.*, 2009) and a potential (non-cytoplasmic) multi-heme cytochrome domain (see Supplementary Fig. S11B). This protein could be part of an additional electron transport complex that directly interacts with the reduced periplasmic cytochrome pool and, possibly via HdrB, reduces DsrC or transfers electrons onto cytoplasmic electron transfer proteins.

Possible mechanisms for syntrophic growth in AOM via direct electron transfer

Microbial syntrophy can occur by transfer of a molecular intermediate such as hydrogen or formate that is produced by a syntrophic metabolizer e.g. a fermenting bacterium and scavenged by a single or multiple partners that oxidize the compound. The activity of the latter prevents product inhibition (McInerney *et al.*, 2009). Alternatively, some organisms have the capability to directly transfer electrons (Summers *et al.*, 2010; Rotaru *et al.*, 2014). Consequently, common features such as systems for reverse electron flow, hydrogenases, formate dehydrogenases, pili and outer membrane cytochromes have been highlighted in the genomes of syntrophic metabolizers (Sieber *et al.*, 2012). *Ca*. D. auxilii grows as syntrophic partner of ANME-1 archaea, both in the environment and *in vitro* (Holler *et al.*, 2011; Wegener *et al.*, 2015). Formate can be excluded as substrate of *Ca*. D. auxilii as it does not grow on formate and its genome does not encode a complete

formate dehydrogenase, necessary to metabolize formate. In contrast, *Ca*. D. auxilii grows on hydrogen and could theoretically utilize its hydrogenases during syntrophic growth via interspecies hydrogen transfer. During TAOM, production of molecular intermediates was, however, not observed (Wegener *et al*., 2015). Instead direct electron transfer (DIET) via excreted multi-heme cytochrome c and nanowire-like structures was proposed for the syntrophic coupling in AOM consortia (McGlynn *et al*., 2015; Wegener *et al*., 2015). DIET is the preferred mode of syntrophic interaction between the syntrophic ethanol metabolizer *G. metallireducens* and its product scavenger *G. sulfurreducens* (Summers *et al*., 2010). The two organisms can switch between interspecies hydrogen transfer and DIET, which may indicate that only a few genetic adaptations are required to alternate between the two modes. In TAOM consortia a dense network of nanowire-like structures was observed that might enable direct interspecies electron transfer (Wegener *et al*., 2015). The *Ca*. D. auxilii genome encodes a set of genes required for biogenesis and assembly of type IV pili (HS1_000117, HS1_000600-HS1_000604, HS1_002000, HS1_002454; see also Supplementary Table S7 and S8, and Wegener *et al*., 2015). Although type IV pili may have various functions including attachment, they seem to play a crucial role in mediating DIET in syntrophically-growing dual-species *Geobacter* consortia (Summers *et al*., 2010). Recent studies indicated that the *Geobacter*-specific geopilins are self-conductive and that the PilA protein contains aromatic amino acids that are the key to electron transport along pili via delocalized charges (Malvankar *et al*. 2014, 2015; Liu *et al*. 2014). Comparison of the amino acid sequences of PilA prepilins from *Ca*. D. auxilii (HS1_000117) and *G. sulfurreducens* revealed that the *Ca*. D. auxilli pilin contains 3 of the 5 aromatic amino acids found in the N-terminal domain of geopilin. Furthermore, in *Geobacter* spp. highly expressed multi-heme c-type cytochromes (OmcS) were proposed to play an important role in electron transfer. *Ca*. D. auxilii lacks this specific cytochrome, but 24 c-type cytochromes were identified of which 10 have orthologous genes in the *G. sulfurreducens* genome and could possibly fulfill similar functions. Three potentially secreted multi-heme c-type cytochromes were related to OmcT (HS1_000545, HS1_000649, HS1_000650), which in *G. sulfurreducens* was suggested to be involved in DIET. Further, seven multi-heme c-type cytochrome encoding genes [HS1_000540 (10 heme), HS1_000543 (12 heme), HS1_000544 (12 heme), HS1_000545 (7 heme), HS1_000548 (7 heme), HS1_000555 (26 heme), HS1_000556 (16 heme)] were located in a large cluster together with other genes, including one encoding an outer-membrane channel cytochrome c [HS1_000541 (1 heme)], related to OmcL of *G. sulfurreducens*, and two encoding lipoproteins (see also Supplementary Table S7 and S8, and Wegener *et al*., 2015). Although the mechanisms of extracellular electron transfer by *Ca*. D. auxilii remain unknown, these cytochromes may be candidates for the extracellular transfer of electrons between pili and outer-membrane and the channeling of electrons into the periplasm via a porin outer-membrane protein. Once transferred to the periplasmic cytochrome pool electrons may be delivered to membrane-bound electron transport complexes via a cytochrome-interacting periplasmic subunit (see above) and subsequently fuel sulfate reduction. *Ca*. D. auxilii could possibly utilize the same redox components to pass electrons between the periplasmic cytochrome pool and cytoplasmic sulfate reduction complexes during DIET-based syntrophic and hydrogenotrophic growth (Fig. 4). This would allow a rather quick transition between both growth modes and may explain its fast response to hydrogen as alternative substrate. Syntrophic growth via DIET would circumvent hydrogenases, hence during syntrophic growth in AOM *Ca*. D. auxilii would not reduce ferredoxin via electron bifurcation at the MvhADG/HdrABC complex. Under these conditions ferredoxin reduction could be driven by proton translocation at the reverse working Rnf complex (see above).

Furthermore, flagella have previously been reported to be an important feature of syntrophy establishment (Shimoyama *et al*., 2009). *Ca*. D. auxilii includes in its genome an almost complete set of genes for flagella assembly and movement (HS1_000713-HS1_000715, HS1_000723-HS1_000730, HS1_000732-HS1_000750, HS1_000753-HS1_000763). Although not observed during growth in consortia (Wegener *et al*., 2015) or in the solitary growth mode in the enrichment on hydrogen (Fig. 2D), flagella might be important to initiate the contact between *Ca*. D. auxilii and ANME-1, or other suitable syntrophic partners. The *Ca*. D. auxilii genome further contains a variety of genes encoding for chemotaxis and response regulation, which possibly play a role in interspecies signaling during syntrophic growth or syntrophy establishment.

Carbon and nitrogen metabolism

Autotrophic carbon fixation in *Ca*. D. auxilii likely proceeds via the reductive tricarboxylic (citric) acid (rTCA) cycle as the complete enzyme set is encoded in its draft genome. In contrast only an incomplete set of genes for carbon fixation via the Wood-Ljundahl pathway (reductive acetyl CoA pathway) was identified, lacking the key enzyme of this pathway, the carbon monoxide dehydrogenase/acetyl CoA synthase. The rTCA cycle which forms one molecule acetyl CoA from the fixation of two molecules of CO_2, is a central metabolic pathway in the cell that generates precursors for lipid and protein biosynthesis (Fuchs, 2011). In sulfate reducers this mechanism of carbon fixation was first described in the hydrogenotrophic *Desulfobacter*

hydrogenophilus (Schauder *et al*., 1987). In the *Ca*. D. auxilii genome the key enzymes of the rTCA cycle, fumarate reductase (HS1_001279, HS1_001733, HS1_001734, HS1_001735), ferredoxin-dependent 2-oxoglutarate oxidoreductase (HS1_001275-HS1_001277) and ATP citrate lyase (HS1_001265-HS1_001266) are encoded in one cluster together with genes for other enzymes of the cycle (HS1_001263, HS1_001268-HS1_001271, HS1_001275, HS1_001281-HS1_001282). This cluster also comprises genes encoding a heterodisulfide reductase (HdrABC, HS1_001272-HS1_001274), adjacent to the ferredoxin-dependent 2-oxoglutarate oxidoreductase genes. The potential electron bifurcating function of Hdr within the MvhADG/HdrABC enzyme complex (Buckel and Thauer, 2013) may provide reduced ferredoxin to the 2-oxoglutarate oxidoreductase during hydrogenotrophic growth. As indicative from the draft genome, *Ca*. D. auxilii converts the product of the rTCA cycle, acetyl CoA, further to pyruvate in a ferredoxin-dependent reductive carboxylation reaction that leads to the fixation of another molecule of CO_2. Genes encoding the responsible enzyme, pyruvate ferredoxin oxidoreductase (HS1_001566, HS1_001571-HS1_001573), were observed in a cluster with genes for an aldehyde ferredoxin reductase (HS1_001562, HS1_001567) two proteins containing 4Fe-4S ferredoxin (HS1_001563, HS1_001568) and proteins with similarity to HdrA (HS1_001564-HS1_001565), HdrB (HS1_001570) and HdrC (HS1_001569). These proteins could be involved in electron transfer reactions and regeneration of reduced ferredoxin. Genes for further conversion of pyruvate to oxalacetate, either via phosphoenolpyruvate (PEP; PEP synthase, HS1_001176 and PEP carboxylase, HS1_002476-HS1_002477) or directly (pyruvate carboxylase, HS1_000172), were present and link carbon fixation to carbohydrate biosynthesis via gluconeogenesis. Although growth of *Ca*. D. auxilii on acetate was not observed, its genome encodes genes for the conversion of acetate to acetyl CoA by acetyl CoA synthetase (HS1_001676, HS1_001693).

Ammonium is likely to be used as inorganic nitrogen source by *Ca*. D. auxilii. Its genome encodes glutamine synthetase (HS1_000233) for the condensation of ammonium and glutamate to glutamine and glutamate synthase (HS1_001956-HS1_001957) to further convert glutamine and 2-oxoglutarate to yield two glutamate molecules. Genes encoding enzymes to catalyze the formation of ammonium from nitrate, nitrate reductase and nitrite reductase, were not found. Further, genes for a nitrogenase complex were not identified, only two genes for a nitrogen fixation protein (*nif*U, HS1_000655, HS1_001433) were present. This confirms earlier studies which indicated that partner bacteria in AOM consortia do not fix molecular nitrogen but assimilate ammonia (Dekas *et al*., 2009).

Implications for the lifestyle of Ca. D. auxilii *in the environment*

In solitary growth mode in our enrichment, *Ca*. D. auxilii thrives as an obligatory thermophilic, hydrogenotrophic and autotrophic sulfate reducer. However, in natural hydrothermally heated hydrocarbon-rich sediments as well as in thermophilic methane-amended enrichments, *Ca*. D. auxilii cells generally appear to be associated with ANME-1 (Fig. 1), implying that close proximity is crucial for dual-species syntrophic growth (Holler *et al*., 2011). A tight cell-to-cell association seems characteristic for DIET-performing syntrophic consortia. As previously shown in the *Geobacter* dual-species consortium, the two partners require direct contact; a partner capable of alternating between hydrogen uptake and DIET would only aggregate during DIET but not during interspecies hydrogen transfer (Summers *et al*., 2010; Rotaru *et al*., 2014). Despite *Ca*. D. auxilii's inability to utilize hydrocarbons, highly affiliated 16S rRNA gene sequences were also detected in anaerobic enrichments with short-chain hydrocarbons as sole energy source (Kniemeyer *et al*., 2007; Adams *et al*., 2013). Hence, in its natural environment, *Ca*. D. auxilii may not be restricted to TAOM syntrophy, but may act as syntrophic partner to a variety of thermophilic organisms, which lack complete oxidative pathways. Its fast (within a few days) response to hydrogen addition together with its rather small genome size indicates that switching between solitary or consortial growth does not require major transformations in the proteome, but may be mediated by similar redox components and enzyme complexes. The flexibility to transition between growth strategies might be of selective advantage in dynamic hydrothermal systems and allows *Ca*. D auxilii to thrive in changing substrate conditions. Hence, in hydrothermal sediments *Ca*. D. auxilii therefore may also grow non-syntrophically using naturally available hydrogen as the energy source for sulfate reduction. However, hydrogen concentrations in Guaymas Basin sediments generally do not exceed some μM (Welhan and Lupton, 1987) whereas methane concentrations are orders of magnitude higher, which explains the growth of *Ca*. D. auxilii primarily in AOM consortia in Guaymas Basin sediments.

Description of 'Candidatus Desulfofervidus auxilii*' and 'Candidatus* Desulfofervidaceae*'*

'*Candidatus* Desulfofervidus auxilii' (De.sul.fo.fer'vi.dus, N.L. prefix Desulfo used in taxonomic names for sulfate-reducing bacteria, *fervidus* L. adj. hot, L. n. the hot one, N.L. n. *Desulfofervidus* hot sulfate reducer; au.xi' li.i, L. neut. n. *auxilium* help/support, *auxilii*, L. gen. n. of help/support indicating that the organism is capable of a syntrophic life style).

The bacterium was enriched from a thermophilic anaerobic methane-oxidizing enrichment obtained with hydrothermal sediments of the Guaymas Basin, Gulf of California, Mexico. The bacterium grows chemolithoautotrophically with sulfate and hydrogen in a temperature range between 50°C and 70°C, optimal at 60°C. No heterotrophic growth was observed. Syntrophic growth (chemoorganoautotrophic) is observed on methane with thermophilic ANME-1 archaea. Cell morphology is rod shaped with a length of 1.0–2.0 μm and width of 0.5–1.0 μm. The bacterium is proposed to belong to the *Candidatus* Desulfofervidaceae (-*aceae* ending to denote a family), a novel family of sulfate-reducing bacteria tentatively placed in the *Deltaproteobacteria*.

Experimental procedures

Enrichment and maintenance of Ca. D. auxilii

Ca. D. auxilii was obtained from a sediment-free, thermophilic (60°C) AOM enrichment from Guaymas Basin sediments (Gulf of California) (see Holler *et al*., 2011). It has been separated from its methanotrophic partner by dilution to extinction series with sulfate and hydrogen as sole energy sources. Dilution to extinction series were prepared in 20 ml Hungate tubes filled with 10 ml artificial seawater medium for sulfate-reducing bacteria modifed from Widdel and Bak (1992) containing the salts (in mM) KBr (0.76), KCl (8.05), $CaCl_2$*$2H_2O$ (10.00), $MgCl_2$*$6H_2O$ (27.89), $MgSO_4$*$7H_2O$ (27.60), NaCl (541.00), $NaHCO_3$ (30.00), NH4Cl (4.67), KH_2PO4 (1.47), and the following solutions (1 ml per l): non-chelated trace element mixture, vitamin mixture, riboflavin solution, vitamin B12 solution, selenite-tungsten solution. Medium was reduced with Na_2S (0.5 mM) and adjusted to a pH of approximately 7.3; for details on media preparation and composition of trace and vitamin solutions see Widdel and Bak (1992). Hungate tubes were supplied with a 250 kPa H_2:CO_2 (80:20) headspace. Dilution series were inoculated with 10% of the anaerobic methanotrophic enrichment and serial dilutions of 1:10 were performed resulting in effective dilutions from 10^2 to 10^{10}. To determine microbial sulfate reduction, sulfide concentration in the medium was repeatedly measured using a colorimetric test (Cord-Ruwisch, 1985). After three months the highest active dilutions were analysed for the presence of *Ca*. D. auxilii cells. The purest enrichments were maintained by transfer into fresh medium (5%–10% inoculum). The latter procedure was repeated when sulfide concentration exceeded 15 mM.

DNA extraction, gene amplification and clone library construction

DNA was extracted from 40 ml of the thermophilic AOM enrichment (50°C and 60°C) and from 100 ml of *Ca*. D. auxilii culture following the protocol by Zhou *et al*. (1996). For 16S rRNA gene amplification the bacterial specific primer set GM3 and GM4 was employed (Muyzer *et al*., 1995). The archaeal specific primer pair Arch20F (Massana *et al*., 1997) and Arch958R (DeLong, 1992) was used to identify the archaeal contaminant in the *Ca.* D. auxilii culture. The *dsr*A gene encoding dissimilatory sulfate reductase subunit A was amplified using the primer set DSR1Fmix (containing DSR1F, DSR1Fa, DSR1Fb, DSR1Fc, DSR1Fd) (Wagner *et al*., 1998; Loy *et al*., 2004; Zverlov *et al*., 2005) and DSR1334R (Santillano *et al*., 2010). Polymerase chain reaction (PCR) was performed in a 20 μl reaction volume, containing 0.5 μM of each primer, 200 μM of each deoxyribonucleoside triphosphate, 6 μg bovine serum albumin, 1x PCR buffer (5'Prime, Hamburg, Germany), 0.25U Taq DNA Polymerase (5'Prime) and 1 μl of template (20–30 ng). The cycle conditions were as follows: initial step at 95°C for 5 min; 26 cycles, each at 95°C for 1 min, 46°C (GM3/GM4), 58°C (Arch20F/Arch958R) or 52°C (DSR1Fmix/DSR1334R) for 1.5 min, and 72°C for 3 min; and final step at 72°C for 10 min. PCR amplicons from three reactions were pooled, purified and concentrated using the QIAquick PCR Purification Kit (Qiagen, Hilden, Germany), gel excised and purified again using the QIAquick Gel Purification Kit (Qiagen) according to the manufacturer's recommendations. Ligation was carried out with the pGEM-T Easy vector system (Promega, Madison, WI, USA) followed by transformation of *Escherichia coli* One Shot Top10 cells (Invitrogen, Carlsbad, CA, USA) according to the manufacturer's recommendations. Clones were screened using the M13F/R primer pair and a standard PCR procedure. Positive inserts were sequenced using ABI BigDye Terminator chemistry and an ABI377 sequencer (Applied Biosystems, Foster City, CA, USA). The PCR product obtained with the archaeal-specific primer pair was purified and sequenced directly.

Probe design

An oligonucleotide probe specifically targeting *Ca*. D. auxilii, probe HotSeep1_1465 (probe sequence 5'-CCCAAGGUGUGGUCGGCG-3') was designed using the probe design tool in the ARB software package (Ludwig *et al*., 2004). The probe was *in silico* tested for sensitivity (target group hits) and specificity (outgroup hits) with the ARB probe match tool (Quast *et al*., 2013). Probe HotSeep1_1465 covers sequences currently assigned to the *Ca*. D. auxilii cluster (97% similarity threshold) with the exception of three sequences (NCBI acc. no.'s KJ569680, FR682643, FR682645; compare Supplementary Table S1) and has at least one mismatch to non-target group sequences (sequences less than 97% similar to the *Ca*. D. auxilii cluster). The oligonucleotide probe (HRP labeled) was synthesized by Biomers (Ulm, Germany). The stringency of the newly designed probe was tested in a CARD-FISH (catalyzed reporter deposition fluorescence *in situ* hybridization) experiment by increasing the formamide concentration in the hybridization buffer from 0% to 70%.

Catalyzed reporter deposition fluorescence in situ hybridization

CARD-FISH was applied to detect *Ca*. D. auxilii cells in AOM enrichments and to repeatedly analyse the purity of *Ca*. D. auxilii cultures. Cells for CARD-FISH were fixed in 2% formamide for 2 h at room temperature and filtered onto polycarbonate filters (0.2 μm pore size, 25 mm diameter, GTTP Millipore, Germany). CARD-FISH was performed

following the standard procedure as described previously (Pernthaler and Amann, 2004) with some modifications. In short: filters were embedded in 0.2% low melting agarose prior to the CARD-FISH procedure. Optimized cell wall permeabilization for probe HotSeep-1_1465 was achieved with lysozyme treatment for 7 min at 37°C [10 mg ml^{-1} lysozyme, lyophilized powder (SigmaAldrich) in 0.1 M Tris–HCl, 0.05 M EDTA, pH 8] followed by proteinase K digestion for 2 min at RT [4.5 mU ml^{-1} proteinase K (Merck) in 0.1 M Tris-HCl, 0.05 M EDTA and 0.5 M NaCl, pH 8]. Endogenous peroxidases were inactivated with 0.15% H_2O_2 in methanol (30 min, RT). For hybridization the following oligonucleotide probes were applied with respective formamide concentration (according to original publication or derived from the melting curve for probe HotSeep-1_1465): EUB338I-III, 35%, Arch915, 35%, ANME-1-350, 40%, HotSeep-1_1456, 35%. Catalyzed reporter deposition was performed using tyramides labelled with the fluorochromes Alexa Fluor 594 or Alexa Fluor 488. When performing double hybridizations (e.g. for the AOM consortia) the peroxidase enzymes of the first hybridization were inactivated with 0.3% H_2O_2 in methanol (30 min, RT) prior to the application of the HRP labeled probe in the second hybridization. For archaeal cell wall permeabilization only 7 min lysozyme at 37°C was used as proteinase K treatment resulted in damage of archaeal cells. Hence, in dual CARD-FISH experiments targeting HotSeep-1 and *Archaea* permeabilization was restricted to lysozyme treatment resulting in less bright signals in *Ca.* D. auxilii cells. Samples were stained with DAPI (40,60-diamidino-2-phenylindole) and visualized using epifluorescence microscopy.

Physiological experiments

To analyse the response of *Ca*. D. auxilii to different substrates and temperatures 1 ml aliquots of cultures pre-grown at 60°C with sulfate, hydrogen and carbon dioxide were inoculated to 20 ml Hungate tubes filled with 10 ml artificial seawater medium for sulfate-reducing bacteria (prepared after Widdel and Bak, 1992; see above). The medium and/or headspace composition was modified with respect to electron donor, electron acceptor/sulfur compound and carbon source to be tested (see below). Sulfate-reducing activity was determined by measuring the sulfide concentration in the medium using the copper-sulfide formation assay (Cord-Ruwisch, 1985).

To test the temperature range and optimum of sulfate-reducing activity, cultures were incubated between 20°C and 80°C (nine temperatures: 20°C, 27°C, 37°C, 50°C, 55°C, 60°C, 65°C, 70°C and 80°C; with triplicates for each temperature). The incubations were provided with 28 mM sulfate and a 250 kPa H_2:CO_2 (80:20) headspace. Sulfide production at each temperature was determined over a period of 3 weeks.

To test an influence of organic substrates (carbon sources) cultures were incubated with 28 mM sulfate and 200 kPa H_2:CO_2 (80:20) plus the potential substrate: formate, acetate, pyruvate, lactate, propionate, benzoate, dicarboxylic acid mixture (succinate, fumarate, malate), methanol, ethanol, glucose, fructose; all 2 mM, peptone and yeast extract; both 0.01% (w/v), carbon monoxide, methyl sulfide; both 10 kPa or methane, propane and butane; all 100 kPa. CO_2 was present as additional carbon source in all incubations. Control experiments were performed under standard conditions with CO_2 as sole carbon source. All substrates were tested in duplicates and incubation was performed at 60°C. The sulfide production was determined over a period of 3 weeks.

To test activity of *Ca*. D. auxilii on alternative electron donors substrates were added to incubations containing sulfate (28 mM) and a N_2:CO_2 (8:2) headspace, except gaseous electron donors (see below). Formate, acetate, pyruvate, lactate, propionate, benzoate, dicarboxylic acid mixture (succinate, fumarate, malate), methanol, ethanol, glucose, fructose were supplied in concentration of 10 mM, peptone and yeast extract as 0.1% (w/v). The following gaseous substrates were tested in kPa: methyl sulfide (10), carbon monoxide (10), methane (100), propane (100) and butane (100). Control experiments were performed under standard conditions with hydrogen as sole electron donor [250 kPa H_2:CO_2 (80:20)]. All substrates were tested in duplicates and incubation was performed at 60°C with sulfide production measured over 3 weeks and up to three month for incubations supplemented with hydrocarbons.

At the end of substrate tests the number of *Ca*. D. auxilii and archaeal cells was determined by counting CARD-FISH-stained cells hybridized with probe HotSeep-1_1456 or Arch915.

The capability to utilize alternative sulfur compounds as electron acceptors or to disproportionate them was tested in sulfate-free incubations supplemented with either sulfite (0.5 mM), thiosulfate (5 mM), sulfate (20 mM), elemental sulfur and colloidal sulfur. In disproportionation experiments the headspace contained 250 kPa N_2:CO_2 (80:20) while in experiments testing for the capability of reduction hydrogen was supplied as electron donor [250 kPa H_2:CO_2 (80:20)]. Sulfide production was measured over 3 weeks.

Growth characteristics were determined from replicate cultures (7.5% inoculum) incubated in 256 ml bottles containing 150 ml artificial seawater medium for sulfate reducing-bacteria (Widdel and Bak, 1992; see above) and a 250 kPa H_2:CO_2 (80:20) headspace. To measure inorganic carbon fixation in a ^{14}C-DIC radiotracer assay replicates (3 of 6 cultures) were spiked with ^{14}C-DIC (~5.4 kBq). Controls were supplied with a N_2:CO_2 headspace (80:20; 2 replicates, 1 ^{14}C spiked, 1 non-spiked). To provide an abiotic control a sterilized (121°C, 25 min) culture aliquot served as inoculum (2 replicates, 1 spike ^{14}C spiked, 1 non-spiked). All incubations were performed at 60°C. Incubations were sampled repeatedly for sulfide (copper sulfide formation assay) and sulfate (ion chromatography) concentrations, for DIC concentrations, for ^{14}C-tracer content and for cell counts over a period of 5 weeks. To measure carbon fixation aliquots of spiked cultures (3–5 ml volume) were blotted on filters (0.2 μm pore size, 25 mm diameter, GSWP). Inorganic carbon was removed via exposure to HCl atmosphere and fixed radiocarbon was determined by scintillation counting. The total carbon fixation was calculated as ^{14}C uptake into particulate organic carbon multiplied by total DIC [^{14}C-POC (kBq $ml^{-1}_{culture}$)/^{14}C-total (kBq $ml^{-1}_{culture}$) × DIC (mmol $ml^{-1}_{culture}$)]. Cell numbers were determined from non-labelled replicates by counting DAPI-stained cells to obtain total cell numbers and specific CARD-FISH-stained cells to determine the fraction of *Ca*. D. auxilii cells.

Scanning electron microscopy

Culture aliquots of *Ca*. D. auxilii were blotted onto gold/palladium sputtered polylysine coated glass slides and single TAOM aggregates were picked from the enrichment culture. Samples were dehydrated in an ethanol series, dried and mounted on electrically conductive, adhesive tags (Leit-Tab; Plano GmbH, Wetzlar, Germany). Specimens were investigated with a FEI environmental field emission SEM Quanta 250 FEG (FEI, Eindhoven, Netherlands) at electron energy of 2 keV using the Everhart-Thornley secondary electron detector (ETD).

Atomic force microscopy

Samples were retrieved from the supernatant of a TAOM enrichment, fixed in 20 g l^{-1} formaldehyde for 30 min at RT and directly filtered onto polycarbonate filters (0.2 μm pore size, 25 mm diameter, GTTP, Millipore, Germany), sputtered with a gold palladium (20%/80%) layer (~ 40 nm). Filters were stored at −20°C or directly analysed using an atomic force microscope (AFM) (NT-MDT Co., Russia) in semi-contact mode with a gold coated silicon cantilever (NSG10). Images were processed using NT-MDT Image Analysing software, version 3.5. Image colour and contrast was optimized using conventional image processing software (Adobe Photoshop CS5, version 12.0.4).

Metagenome sequencing and assembly

Genomic DNA was extracted according to the protocol by Zhou *et al*. (1996) from a cell pellet of 100 ml *Ca*. D. auxilii culture (harvested by centrifugation at 5000×g for 15 min, 4°C). 2 μg of high molecular weight DNA was subjected to fragment library construction using the Nextera Mate Pair Library Preparation Kit (Illumina), following the Gel-Plus protocol of the manufacturer's user guide. DNA fragments of approx. 5–8 kb were extracted from a preparative gel prior to circularization. The mate pair library was sequenced on a MiSeq instrument (MiSeq, Illumina) in a 2 × 300 bases paired end run.

To estimate the taxonomic composition of the metagenomic dataset raw reads were mapped to the SILVA database (release 119) (Quast *et al*., 2013) using bbmap v.35. implemented in phyloflash v.1.5 with minimum identity of 95%. For quantification only unambiguously mapped reads were counted. Nearly full length 16S rRNA gene sequences assembled by phyloflash were classified as HotSeep-1 (99.4% identity, 1530 bp, coverage 107.5) and *Archaeoglobus fulgidus* (98% identity, 1035 bp, coverage 2.5).

Quality of raw read data was assessed using FastQC and raw reads were processed, including adapter clipping, trimming of bases with quality below Q30 and removal of reads shorter 50 bp using bbduk2 (bbmap v.35). *De novo* assembly was performed with quality controlled mate pair reads using the SPAdes genome assembler v. 3.5.0. (Bankevich *et al*., 2012) with default values for k and the option for high quality mate pairs (–hqmp). In total 2577039 bp were assembled into 57 contigs >1000 kb, representing 31 scaffolds (N50 2540211 bp). The largest, final scaffold of 2540211 bp was used for all further analysis. Small and low coverage scaffolds (on average <5 kb length and <2x coverage) were excluded from the analysis.

Completeness of the draft genome assembly was evaluated with checkM (Parks *et al*., 2015) using the lineage-specific workflow. In addition, completeness was also estimated with the AMPHORA2 package using the 31 bacterial marker genes (Wu and Scott, 2012).

ORF prediction and annotation

Gene prediction was carried out using the Glimmer3 (Delcher *et al*., 2007) software package. Ribosomal RNA genes were detected by using the RNAmmer 1.2 software (Lagesen *et al*., 2007) and transfer RNAs by tRNAscan-SE (Lowe and Eddy, 1997). Batch cluster analysis was performed by using the GenDB (version 2.2) system (Meyer *et al*., 2003). Annotation and data mining were done with the tool JCoast, version 1.7 (Richter *et al*., 2008), using observations from similarity searches against several sequence databases (NCBI-nr, Swiss-Prot, KEGG-Genes, genomesDB) and to the protein family databases InterPro (Mulder *et al*., 2005) and Pfam (Bateman *et al*., 2004) for each coding region. Predicted protein coding sequences were automatically annotated by the software tool MicHanThi (Quast, 2006). Briefly, the MicHanThi software interferes gene functions based on similarity searches against the NCBI-nr (including Swiss-Prot) and InterPro databases using fuzzy logic. The annotation of proteins highlighted within the scope of this study was subject of manual inspection. For all observations regarding putative protein functions, an *expectation (E)*-value cut-off of 10^{-5} was applied. For proteins of interest the subcellular localization was predicted by PSORTb v.3.0.2. (Yu *et al*., 2010) and transmembrane helices were identified by TMHMM scan v.2.0 (Krogh *et al*., 2001). Further, for selected proteins signal peptides and alternative secretion (without signal peptide) were predicted with SignalP 4.1 (Petersen *et al*., 2011) and SecretomP 2.0 (Bendtsen *et al*., 2005) respectively. Potential c-type cytochromes and type IV pili proteins were identified by protein domain models related to cytochrome c or type IV pili respectively. For cytochromes the number of hemes was derived from the number of detected CXXCH motifs, which are indicative for heme-binding sites.

Comparison of the shared gene content by reciprocal best matches

Determination of the shared orthologous gene content has been performed by a blast 'all-versus-all' search between selected organisms (members of the *Deltaproteobacteria*, *Thermodesulfobacteria* and *Nitrospira*). Reciprocal best matches were counted by a blast result with *E*-values of $<10^{-5}$ each and a subject coverage of over 65%.

Taxonomic distributions

To analyse the *Ca*. D. auxilii genome for the taxonomic distribution of best matches the genome was compared against the genomesDB database (Richter *et al*., 2008), an in house protein database based on the NCBI Reference Sequence database (RefSeq) containing protein sequences from all sequenced bacterial and archaeal genomes. Each predicted protein of *Ca*. D. auxilii was searched against the genomesDB

and the best match was recorded on phyla and species level. Only those proteins with significant hits (*E*-value $>10^{-5}$) were considered.

Functional classification with KEGG

For metabolic pathway identification, genes were searched for similarity against the KEGG database. A match was counted if the similarity search resulted in an *E*-value below 10^{-5}. All occurring KO (KEGG Orthology) numbers were mapped against KEGG pathway functional hierarchies and statistically analysed.

Functional classification with COG

All predicted ORFs were also searched for similarity against the COGs database (Tatusov *et al*., 2003). A match was counted if the similarity search resulted in an *E*-value below 10^{-5}.

16S rRNA gene sequence analysis

The genomic 16S rRNA gene sequence of *Ca*. D. auxilii was compared to the NCBI database of reference sequences (rna-RefSeq, containing curated, non-redundant sequences; 17765 database entries, 15.10.2015) and the NCBI nucleotide collection database (nt/nr, including environmental sequences; 28723871 database entries, 27.10.2014) using NCBI blastn (2.2.30) (Zhang *et al*., 2000) under default settings. Phylogenetic analysis was performed using the ARB software package (Ludwig *et al*., 2004) and the SILVA database (release 119) (Quast *et al*., 2013). Sequence selection for analysis was based on the initial blast hits to *Ca*. D. auxilii (see above); the 100 top scoring rna-RefSeq database entries (query coverage >85%) were included and used as references to guide further sequence selection from related classes/phyla. In addition, sequences in the nt/nr database with similarity >90% to *Ca*. D. auxilii as well as sequences obtained from the thermophilic Guaymas Basin AOM enrichments and the *Ca*. D. auxilii culture were considered. The *Ca*. D. auxilii sequence cluster was defined based on 97.5% sequence similarity. Similarity was determined from a similarity matrix (neighbour-joining algorithm) considering nearly full length sequences (>1300 bp). For phylogenetic reconstruction 654 nearly full length sequences (>1300 bp) covering several bacterial classes and phyla, including *Deltaproteobacteria*, *Thermodesulfobacteria* and *Nitrospira* were aligned using the SINA aligner implemented in ARB (Pruesse *et al*., 2012) and the alignment was manually curated. Distance matrix trees were calculated with the neighbour-joining algorithm (Saitou and Nei, 1987) and Jukes Cantor correction. Maximum likelihood based trees were calculated using RAxML (version 8.0.26) (Stamatakis, 2006) with GTRGAMMA as nucleotide substitution model or PhyML with GTR as nucleotide substitution model. A base frequency filter was employed for each tree calculation to consider only alignment regions which are 50% conserved. 1000 bootstrap replicates were used to estimate branch supports.

23S rRNA gene sequence analysis

Phylogenetic analysis of the genomic 23S rRNA of *Ca*. D. auxilii was performed with the SILVA LSU reference database (release 119) (Quast *et al*., 2013) and the ARB software package (Pruesse *et al*., 2012). The sequence alignment was manually curated and phylogenetic trees were calculated with the maximum likelihood algorithm using RAxML (version 8.0.26) (Stamatakis, 2006) with GTRGAMMA as nucleotide substitution model or PhyML with GTR as nucleotide substitution model. To include only conserved alignment regions a 50% base frequency filter was employed. Branch support was estimated by 100 bootstrap replicates.

DsrA sequence analysis

For functional gene based phylogenetic analysis the *dsr*A gene sequence of *Ca*. D. auxilii was obtained from its genome sequence. Additional *dsr*A gene sequences were retrieved from the thermophilic AOM enrichments (50°C and 60°C) and the *Ca*. D. auxilii culture. Related sequences were obtained from the NCBI-nr database using a blastp search of the genomic DsrA amino acid sequence of *Ca*. D. auxilii. For phylogenetic analyses sequences were added to the *dsr*AB/DsrAB database constructed by Müller *et al*. (2014) and aligned using the ARB software package (Ludwig *et al*., 2004). A phylogenetic tree was calculated from 256 aligned amino acid sequences with the maximum likelihood algorithm (RAxML version 8.2.4.) using the rate distribution model PROTGAMMA and LG as substitution matrix. The best suited substitution model was determined by RAxML using the –m PROTGAMMAAUTO option. Employing a 30% base frequency filter to exclude highly variable regions a total of 260 alignment positions were included in the phylogenetic reconstruction. Branch support was estimated from 100 bootstrap replicates.

Single copy gene analysis

Single copy gene analysis of *Ca*. D. auxilii was carried out with the AMPHORA2 software package which uses a set of 31 universal bacterial single copy genes as marker (Wu and Scott, 2012). Single copy genes were identified from the nucleotide sequence, aligned with references and assigned to phylotypes by maximum likelihood algorithm. To reconstruct the phylogenetic affiliation of *Ca*. D. auxilii on the level of multiple single copy genes the AMPHORA2 MarkerScanner and MarkerAlignTrim tools were used to identify, align and trim single copy genes present in *Ca*. D. auxilii and selected reference genomes. As references genomes of organisms that had been used in 16S rRNA gene based phylogenetic analysis (if available) and additionally those that were of interest based on the results from comparative genomic analysis were included. A marker gene was excluded if not present in all analysed genomes resulting in ubiquitous 19 single copy genes (Supplementary Table S2). The trimmed protein alignments of each marker were concatenated using SequenceMatrix (Vaidya *et al*., 2011) and phylogenetic trees were calculated from the multi-protein alignment (2857 positions) using the maximum likelihood algorithm (RAxML version 8.2.4.) applying PROTGAMMA and LG as substitution model and 100 bootstrap replicates to estimate branch

supports (Stamatakis, 2006). The best suitable substitution model for the concatenated multi gene alignment was selected by using the –m PROTGAMMAAUTO option provided by RAxML. The iTOL software (Letunic and Bork, 2011) was used for tree visualization.

Nucleotide sequence accession numbers

The Whole Genome Shotgun project has been deposited in INSDC (DDBJ/EBI-ENA/GenBank) under the BioProject PRJNA276404 and the annotated draft genome of *Ca*. D. auxilii is available under accession CP013015. The sequence associated contextual (meta)data are MIxS (Yilmaz *et al*., 2011) compliant. Representative *dsr*A sequences are deposited in INSDC (DDBJ/EBI-ENA/GenBank) under accession numbers KT819174-KT819177.

Acknowledgements

We thank Susanne Menger, Mirja Meiners and Ines Kattelmann for technical assistance and Ulrich Fischer for valuable discussion. We are grateful to Hans G. Trüper, University of Bonn, Germany, for his precious help with the etymology. Furthermore, we thank chief scientist Andreas Teske and the RV ATLANTIS and ALVIN team of cruise AT15-56 in 2009 (NSF Grant OCE-0647633) for providing the initial sediment material. The project was funded by the DFG Leibniz program (to A.B.), the DCO Deep Life program (to G.W.), the Max Planck Society, and the DFG excellence cluster MARUM, Center of Marine Environmental Sciences, Bremen.

References

Adams, M.M., Hoarfrost, A.L., Bose, A., Joye, S.B., and Girguis, P.R. (2013) Anaerobic oxidation of short-chain alkanes in hydrothermal sediments: potential influences on sulfur cycling and microbial diversity. *Front Microbiol* **4:** 110. doi:10.3389/fmicb.2013.00110.

Alazard, D., Dukan, S., Urios, A., Verhe, F., Bouabida, N., Morel, F., *et al*. (2003) *Desulfovibrio hydrothermalis* sp. nov., a novel sulfate-reducing bacterium isolated from hydrothermal vents. *Int J Syst Evol Microbiol* **53:** 173–178.

Anderson, I., Saunders, E., Lapidus, A., Nolan, M., Lucas, S., Tice, H., *et al*. (2004) Genome sequence of the thermophilic sulfate-reducing ocean bacterium *Thermodesulfatator indicus* type strain (CIR29812 T). *Stand Genomic Sci* **6:** 155–164.

Audiffrin, C., Cayol, J., Joulian, C., Casalot, L., Thomas, P., Garcia, J., *et al*. (2003) *Desulfonauticus submarinus* gen. nov., sp. nov., a novel sulfate-reducing bacterium isolated from a deep-sea hydrothermal vent. *Int J Syst Evol Microbiol* **53:** 1585–1590.

Bankevich, A., Nurk, S., Antipov, D., Gurevich, A.A., Dvorkin, M., Kulikov, A.S., *et al*. (2012) SPAdes: a new genome assembly algorithm and its applications to single-cell sequencing. *J Comput Biol* **19:** 455–477.

Bateman, A., Coin, L., Durbin, R., Finn, R.D., Hollich, V., Grif, S., *et al*. (2004) The Pfam protein families database. *Nucleic Acids Res* **32:** 138–141.

Bendtsen, J.D., Kiemer, L., Fausbøll, A., and Brunak, S. (2005) Non-classical protein secretion in bacteria. *BMC Microbiol* **13:** 1–13.

Biddle, J.F., Cardman, Z., Mendlovitz, H., Albert, D.B., Lloyd, K.G., Boetius, A., *et al*. (2011) Anaerobic oxidation of methane at different temperature regimes in Guaymas Basin hydrothermal sediments. *ISME J* **6:** 1018–1031.

Biegel, E., and Müller, V. (2010) Bacterial Na^+-translocating ferredoxin:NAD^+ oxidoreductase. Proc Natl Acad Sci USA **107:** 18138–13142.

Boetius, A., and Wenzhöfer, F. (2013) Seafloor oxygen consumption fuelled by methane from cold seeps. *Nat Geosci* **6:** 725–734.

Boetius, A., Ravenschlag, K., Schubert, C.J., Rickert, D., Widdel, F., Gieseke, A., *et al*. (2000) A marine microbial consortium apparently mediating anaerobic oxidation of methane. *Nature* **407:** 623–626.

Brandis, A., and Thauer, R.K. (1981) Growth of *Desulfovibrio* species on hydrogen and sulphate as sole energy source. *J Gen Microbiol* **126:** 249–252.

Brysch, K., Schneider, C., Fuchs, G., and Widdel, F. (1987) Lithoautotrophic growth of sulfate-reducing bacteria, and description of *Desulfobacterium autotrophicum* gen. nov., sp. nov. *Arch Microbiol* **148:** 264–274.

Buckel, W., and Thauer, R.K. (2013) Energy conservation via electron bifurcating ferredoxin reduction and proton/Na^+ translocating ferredoxin oxidation. *Biochim Biophys Acta* **1827:** 94–113.

Cord-Ruwisch, R. (1985) A quick method for the determination of dissolved and precipitated sulfides in cultures of sulfate-reducing bacteria. *J Microbiol Methods* **4:** 33–36.

Cypionka, H., and Pfennig, N. (1986) Growth yields of *Desulfotomaculum orientis* with hydrogen in chemostat culture. *Arch Microbiol* **143:** 396–399.

Dekas, A.E., Poretsky, R.S., and Orphan, V.J. (2009) Deep-sea archaea fix and share nitrogen in methane-consuming microbial consortia. *Science* **326:** 422–426.

Delcher, A.L., Bratke, K.A., Powers, E.C., and Salzberg, S.L. (2007) Identifying bacterial genes and endosymbiont DNA with Glimmer. *Bioinformatics* **23:** 673–679.

DeLong, E.F. (1992) Archaea in coastal marine environments. *Proc Natl Acad Sci USA* **89:** 5685–5689.

Dowell F., Cardman, Z., Dasarathy, S., Kellermann, M.Y., Lipp, J.S., Ruff, S.E., *et al*. (2016) Microbial communities in methane- and short chain alkane-rich hydrothermal sediments of the Guaymas Basin. *Front Microbiol* **7:** 17. doi:10.3389/fmicb.2016.00017.

Elkins, J.G., Hamilton-Brehm, S.D., Lucas, S., Han, J., Lapidus, A., Cheng, J., *et al*. (2013) Complete genome sequence of the hyperthermophilic sulfate-reducing bacterium *Thermodesulfobacterium geofontis* OPF15^T. *Genome Announc* **1:** 1–2.

Fuchs, G. (2011) Alternative pathways of carbon dioxide fixation: insights into the early evolution of life? *Annu Rev Microbiol* **65:** 631–658.

Grein, F., Ramos, A.R., Venceslau, S.S., and Pereira, I.A.C. (2013) Unifying concepts in anaerobic respiration: insights from dissimilatory sulfur metabolism. *Biochim Biophys Acta* **1827:** 145–160.

Hallam, S.J., Detter, J.C., Rokhsar, D., and Richardson, P.M. (2004) Reverse methanogenesis: testing the hypothesis with environmental genomics. *Science* **305:** 1457–1462.

Hoehler, T.M., Alperin, M,J., Albert, D.B., Martens, S., and Field, A. (1994) Field and laboratory studies of methane

oxidation in an anoxic marine sediment: evidence for a methanogen-sulfate reducer consortium. *Global Biogeochem Cycles* **8:** 451–463.

Holler, T., Widdel, F., Knittel, K., Amann, R., Kellermann, M.Y., Hinrichs, K.-U., *et al.* (2011) Thermophilic anaerobic oxidation of methane by marine microbial consortia. *ISME J* **5:** 1946–1956.

Huntemann, M., Lu, M., Nolan, M., Lapidus, A., Lucas, S., Deshpande, S., *et al.* (2011) Complete genome sequence of the thermophilic sulfur-reducer *Hippea maritima* type strain (MH 2^T). *Stand Genomic Sci* **4:** 303–311.

Jørgensen, B.B., Zawacki, L.X., and Jannascht, H.W. (1990) Thermophilic bacterial sulfate reduction in deep-sea sediments at the Guaymas Basin hydrothermal vent site (Gulf of California). *Deep Sea Res Part A Oceanogr Res Pap* **37:** 695–710.

Kawasumi, T., Igarashi, Y., Kodama, T., and Minoda, Y. (1980) Isolation of strictly thermophilic and obligately autotrophic hydrogen bacteria. *Agric Biol Chem* **44:** 1985–1986.

Kellermann, M.Y., Wegener, G., Elvert, M., Yoshinaga, M.Y., Lin, Y.-S., Holler, T., *et al.* (2012) Autotrophy as a predominant mode of carbon fixation in anaerobic methane-oxidizing microbial communities. *Proc Natl Acad Sci USA* **109:** 19321–19326.

Klein, M., Friedrich, M., Roger, A.J., Hugenholtz, P., Fishbain, S., Abicht, H., *et al.* (2001) Multiple lateral transfers of dissimilatory sulfite reductase genes between major lineages of sulfate-reducing prokaryotes. *J Bacteriol* **183:** 6028–6035.

Kleindienst, S., Ramette, A., Amann, R., and Knittel, K. (2012) Distribution and *in situ* abundance of sulfate-reducing bacteria in diverse marine hydrocarbon seep sediments. *Environ Microbiol* **14:** 2689–2710.

Kniemeyer, O., Musat, F., Sievert, S.M., Knittel, K., Wilkes, H., Blumenberg, M., *et al.* (2007) Anaerobic oxidation of short-chain hydrocarbons by marine sulphate-reducing bacteria. *Nature* **449:** 6–10.

Knittel, K., and Boetius, A. (2009) Anaerobic oxidation of methane: progress with an unknown process. *Annu Rev Microbiol* **6:** 311–334.

Knittel, K., Lemke, A., and Lochte, K. (2003) Activity, distribution, and diversity of sulfate reducers and other bacteria in sediments above gas hydrate (Cascadia Margin, Oregon). *Geomicrobiol J* **20:** 269–294.

Kristjansson, J.K., Ingason, A., and Alfredsson, G.A. (1985) Isolation of thermophilic obligately autotrophic hydrogen-oxidizing bacteria, similar to *Hydrogenobacter thermophiles*, from Icelandic hot springs. *Arch Microbiol* **140:** 321–325.

Krogh, A., Larsson, B., von Heijne, G., and Sonnhammer, E.L. (2001) Predicting transmembrane protein topology with a hidden markov model: application to complete genomes. *J Mol Biol* **305:** 567–580.

Lagesen, K., Hallin, P., Rødland, E.A., Stærfeldt, H., Rognes, T., and Ussery, D.W. (2007) RNAmmer: consistent and rapid annotation of ribosomal RNA genes. *Nucleic Acids Res* **35:** 3100–3108.

Letunic, I., and Bork, P. (2011) Interactive Tree Of Life v2: online annotation and display of phylogenetic trees made easy. *Nucleic Acids Res* **39:** 1–4.

Liu, X., Tremblay, P., Malvankar, N.S., Nevin, K.P., and Lovley, D.R. (2014) A *Geobacter sulfurreducens* strain expressing *Pseudomonas aeruginosa* type IV pili localizes OmcS on pili but is deficient in Fe(III) oxide reduction and current production. *Appl Environ Microbiol* **80:** 1219–1224.

Lowe, T.M., and Eddy, S.R. (1997) tRNAscan-SE: a program for improved detection of transfer RNA genes in genomic sequence. *Nucleic Acids Res* **25:** 955–964.

Loy, A., Küsel, K., Lehner, A., Harold, L., Wagner, M., Ku, K., *et al.* (2004) Microarray and functional gene analyses of sulfate-reducing prokaryotes in low-sulfate, acidic fens reveal cooccurrence of recognized genera and novel lineages. *Appl Environ Microbiol* **70:** 6998–7009.

Ludwig, W., Strunk, O., Westram, R., Richter, L., Meier, H., Buchner, A., *et al.* (2004) ARB: a software environment for sequence data. *Nucleic Acids Res* **32:** 1363–1371.

Malvankar, N.S., Yalcin, S.E., Tuominen, M.T., and Lovley, D.R. (2014) Visualization of charge propagation along individual pili proteins using ambient electrostatic force microscopy. *Nat Nanotechnol* **9:** 1012–1017.

Malvankar, N.S., Vargas, M., Nevin, K., Tremblay, P.-L., Evans-Lutterodt, K., Nykypanchuk, D., *et al.* (2015) Structural basis for metallic-like conductivity in microbial nanowires. *mBio* **6:** e00084–15 doi:10.1128/mBio.00084-15.

Massana, R., Murray, A.E., Preston, C.M., and Delong, E.F. (1997) Vertical distribution and phylogenetic characterization of marine planktonic *Archaea* in the Santa Barbara Channel. *Appl Environ Microbiol* **63:** 50–56.

Matias, P.M., Pereira, I.A.C., Soares, C.M., and Carrondo, M.A. (2005) Sulphate respiration from hydrogen in *Desulfovibrio* bacteria: a structural biology overview. *Prog Biophys Mol Biol* **89:** 292–329.

McGlynn, S.E., Chadwick, G.L., Kempes, C.P., and Orphan, V.J. (2015) Single cell activity reveals direct electron transfer in methanotrophic consortia. *Nature* **526:** 531–535.

McInerney, M.J., Rohlin, L., Mouttaki, H., Kim, U., Krupp, R.S., Rios-Hernandez, L., *et al.* (2007) The genome of *Syntrophus aciditrophicus*: life at the thermodynamic limit of microbial growth. *Proc Natl Acad Sci USA* **104:** 7600–7605.

McInerney, M.J., Sieber, J.R., and Gunsalus, R.P. (2009) Syntrophy in anaerobic global carbon cycles. *Curr Opin Biotechnol* **20:** 623–632.

Meyer, F., Goesmann, A., McHardy, A.C., Bartels, D., Bekel, T., Clausen, J.È., *et al.* (2003) GenDB–an open source genome annotation system for prokaryote genomes. *Nucleic Acids Res* **31:** 2187–2195.

Michaelis, W., Seifert, R., Nauhaus, K., Treude, T., Thiel, V., Blumenberg, M., *et al.* (2002) Microbial reefs in the Black Sea fueled by anaerobic oxidation of methane. *Science* **297:** 1013–1015.

Milucka, J., Ferdelman, T.G., Polerecky, L., Franzke, D., Wegener, G., Schmid, M., *et al.* (2012) Zero-valent sulphur is a key intermediate in marine methane oxidation. *Nature* **491:** 541–546.

Milucka, J., Widdel, F., and Shima, S. (2013) Immunological detection of enzymes for sulfate reduction in anaerobic methane-oxidizing consortia. *Environ Microbiol* **15:** 1561–1571.

Moran, J.J., Beal, E.J., Vrentas, J.M., Orphan, V.J., Freeman, K.H., and House, C.H. (2008) Methyl sulfides as

intermediates in the anaerobic oxidation of methane. *Environ Microbiol* **10:** 162–173.
Mulder, N.J., Apweiler, R., Attwood, T.K., Bairoch, A., Bateman, A., Binns, D., *et al*. (2005) InterPro, progress and status in 2005. *Nucleic Acids Res* **33:** 201–205.
Müller, A.L., Kjeldsen, K.U., Rattei, T., Pester, M., and Loy, A. (2014) Phylogenetic and environmental diversity of DsrAB-type dissimilatory (bi) sulfite reductases. *Int J Syst Evol Microbiol* **9:** 1152–1165.
Muyzer, G., Teske, A., and Wirsen, C.O. (1995) Phylogenetic relationships of *Thiomicrospira* species and their identification in deep-sea hydrothermal vent samples by denaturing gradient gel electrophoresis of 16S rDNA fragments. *Arch Microbiol* **164:** 165–172.
Niemann, H., Lösekann, T., Beer D.D., Elvert, M., Nadalig, T., Knittel, K., *et al*. (2006) Novel microbial communities of the Haakon Mosby mud volcano and their role as a methane sink. *Nature* **443:** 854–858.
Orphan, V.J., Hinrichs, K., Iii, W.U., Paull, C.K., Taylor, L.T., Sylva, S.P., *et al*. (2001a) Comparative analysis of methane-oxidizing archaea and sulfate-reducing bacteria in anoxic marine sediments. *Appl Environ Microbiol* **67:** 1922–1934.
Orphan, V.J., House, C.H., Hinrichs, K., McKeegan, K.D., and DeLong, E.F. (2001b) Methane-consuming archaea revealed by directly coupled isotopic and phylogenetic analysis. *Science* **293:** 484–487.
Parks, D.H., Imelfort, M., Skennerton, C.T., Hugenholtz, P., Tyson, G.W., Centre, A., *et al*. (2015). CheckM: assessing the quality of microbial genomes recoverd from isolates, single cells, and metagenomes. *Genome Res* **25:** 1043–1055.
Pereira, I.A.C., Ramos, A.R., Grein, F., Marques M.C., da Silva, S.M., and Venceslau, S.S. (2011) A comparative genomic analysis of energy metabolism in sulfate reducing bacteria and archaea. *Front Microbiol* **2:** 69. doi:10.3389/fmicb.2011.00069.
Pernthaler, A., and Amann, R. (2004) Simultaneous fluorescence in situ hybridization of mRNA and rRNA in environmental bacteria. *Appl Environ Microbiol* **70:** 5426–5433.
Petersen, T.N., Brunak, S., von Heijne, G., and Nielsen, H. (2011) SignalP 4.0: discriminating signal peptides from transmembrane regions. *Nat Methods* **8:** 785–786.
Pires, R.H., Lourenço, A.I., Morais, F., Teixeira, M., Xavier, A.V., Saraiva, L.M., *et al*. (2003) A novel membrane-bound respiratory complex from *Desulfovibrio desulfuricans* ATCC 27774. *Biochim Biophys Acta* **1605:** 67–82.
Pruesse, E., Peplies, J., Glöckner, F.O., Editor, A., and Wren, J. (2012) SINA: accurate high-throughput multiple sequence alignment of ribosomal RNA genes. *Bioinformatics* **28:** 1823–1829.
Quast, C. (2006) MicHanThi - design and implementation of a system for the prediction of gene functions in genome annotation projects. Diploma Thesis. University of Bremen, Germany.
Quast, C., Pruesse, E., Yilmaz, P., Gerken, J., Schweer, T., Glo, F.O., *et al*. (2013) The SILVA ribosomal RNA gene database project: improved data processing and web-based tools. *Nucleic Acids Res* **41:** 590–596.
Rabus, R., Hansen, T.A., and Widdel, F. (2006) Dissimilatory sulfate- and sulfur-reducing prokaryotes. In: *The Prokaryotes*. Dworkin, M., Falkow, S., Rosenberg, E., Schleifer, K.-H., and Stackebrandt, E. (eds). New York, USA. Springer, pp. 659–768.
Ramos, A.R., Keller, K.L., Wall, J.D., and Pereira, I.A.C. (2012) The membrane QmoABC complex interacts directly with the dissimilatory adenosine 5'-phosphosulfate reductase in sulfate reducing bacteria. *Front Microbiol* **3:** 137. doi:10.3389/fmicb.2012.00137.
Richter, M., Lombardot, T., Kostadinov, I., Kottmann, R., Duhaime, M.B., Peplies, J., *et al*. (2008) JCoast - A biologist-centricsoftware tool for data mining and comparison of prokaryotic (meta)genomes. *BMC Bioinformatics* **9:** 1–9.
Rotaru, A., Malla, P., and Liu, F. (2014) Direct interspecies electron transfer between *Geobacter metallireducens* and *Methanosarcina barkeri*. *Appl Environ Microbiol* **80:** 4599–4605.
Ruff, S.E., Biddle, J.F., Teske, A.P., Knittel, K., Boetius, A., and Ramette, A. (2015) Global dispersion and local diversification of the methane seep microbiome. Proc Natl Acad Sci USA **112:** 4015–4020.
Saitou, N., and Nei, M. (1987) The neighbor-joining method: a new method for reconstructing phylogenetic trees. *Mol Biol Evol* **4:** 406–425.
Santillano, D., Boetius, A., and Ramette, A. (2010) Improved *dsr*A-based terminal restriction fragment length polymorphism analysis of sulfate-reducing bacteria. *Appl Environ Microbiol* **76:** 5306–5311.
Schauder, R., Widdel, F., and Fuchs, G. (1987) Carbon assimilation pathways in sulfate-reducing bacteria II. Enzymes of a reductive citric acid cycle in the autotrophic *Desulfobacter hydrgenophilus*. *Arch Microbiol* **3:** 218–225.
Schmehl, M., Jahn, A., Meyer, A., Hennecke, S., Masepohl, B., Schnppler, M., *et al*. (1993) Identification of a new class of nitrogen fixation genes in *Rhodobacter capsulatus*: a putative membrane complex involved in electron transport to nitrogenase. *Mol Gen Genet* **241:** 602–615.
Shimoyama, T., Kato, S., Ishii, S., and Watanabe, K. (2009) Flagellum mediates symbiosis. *Science* **323:** 1574.
Sieber, J.R., McInerney, M.J., and Gunsalus, R.P. (2012) Genomic insights into syntrophy: the paradigm for anaerobic metabolic cooperation. *Annu Rev Microbiol* **66:** 429–452.
Stamatakis, A. (2006) RAxML-VI-HPC: maximum likelihood-based phylogenetic analyses with thousands of taxa and mixed models. *Bioinformatics* **22:** 2688–2690.
Strittmatter, A.W., Liesegang, H., Rabus, R., Decker, I., Amann, J., Andres, S., *et al*. (2009) Genome sequence of *Desulfobacterium autotrophicum* HRM2, a marine sulfate reducer oxidizing organic carbon completely to carbon dioxide. *Environ Microbiol* **11:** 1038–1055.
Summers, Z.M., Fogarty, H.E., Leang, C., Franks, A.E., Malvankar, N.S., and Lovley, D.R. (2010) Direct exchange of electrons within aggregates of an evolved syntrophic coculture of anaerobic bacteria. *Science* **330:** 1413–1415.
Tatusov, R.L., Fedorova, N.D., Jackson, J.D., Jacobs, A.R., Kiryutin, B., Koonin, E.V., *et al*. (2003) The COG database: an updated version includes eukaryotes. *BMC Bioinformatics* **14:** 1–14.
Teske, A., Hinrichs, K., Edgcomb, V., Gomez, D.V., Kysela, D., Sylva, S.P., *et al*. (2002) Microbial diversity of hydrothermal sediments in the Guaymas Basin: evidence for anaerobic

methanotrophic communities. *Appl Environ Microbiol* **68:** 1994–2007.

Thauer, R.K., Kaster, A., Seedorf, H., and Buckel, W. (2008) Methanogenic archaea: ecologically relevant differences in energy conservation. *Nat Rev Microbiol* **6:** 579–591.

Vaidya, G., Lohman, D.J., and Meier, R. (2011) SequenceMatrix: concatenation software for the fast assembly of multigene datasets with character set and codon information. *Cladistics* **27:** 171–180.

Venceslau, S.S., Lino, R.R., and Pereira, I.A.C. (2010) The Qrc membrane complex, related to the alternative complex III, is a menaquinone reductase involved in sulfate respiration. *J Biol Chem* **285:** 22774–22783.

Venceslau, S.S., Stockdreher, Y., Dahl, C., and Pereira, I.A.C. (2014) The 'bacterial heterodisulfide' DsrC is a key protein in dissimilatory sulfur metabolism. *Biochim Biophys Acta* **1837:** 1148–1164.

Vigneron, A., Cruaud, P., Pignet, P., Caprais, J., Gayet, N., Godfroy, A., *et al.* (2014) Bacterial communities and syntrophic associations involved in anaerobic oxidation of methane process of the Sonora Margin cold seeps, Guaymas Basin. *Environ Microbiol* **16:** 2777–2790.

Wagner, M., Roger, A.J., Flax, J.L., Gregory, A., Stahl, D.A., and Brusseau, G.A. (1998) Phylogeny of dissimilatory sulfite reductases supports an early origin of sulfate respiration. *J Bacteriol* **180:** 2975–2982.

Wegener, G., Niemann, H., Elvert, M., Hinrichs, K., and Boetius A. (2008). Assimilation of methane and inorganic carbon by microbial communities mediating the anaerobic oxidation of methane. *Environ Microbiol* **10:** 2287–2298.

Wegener, G., Krukenberg, V., Riedel, D., Tegetmeyer, H.E., and Boetius, A. (2015) Intercellular wiring enables electron transfer between methanotrophic archaea and bacteria. *Nature* **526:** 587–590.

Wegener, G., Krukenberg, V., Ruff, S.E., Kellermann, M.Y., and Knittel, K. (2016) Metabolic capabilities of microorganisms involved in and associated with the anaerobic oxidation of methane. *Front Microbiol* **7:** 46. doi:10.3389/fmicb.2016.00046.

Welhan, J.A., and Lupton, J.E. (1987). Light hydrocarbon gases in Guaymas Basin hydrothermal fluids: Thermogenic versus abiogenic origin. *Am Assoc Petrol Geol Bull.* **71:** 215–223.

Widdel, F., and Bak, F. (1992) Gram negative mesophilic sulphate-reducing bacteria. In *The Prokaryotes*. Balows, A., Trüper, H.G., Dworkin, M., Harder, W., and Schleifer, K.-H. (eds). New York, USA. Springer, pp. 3352–3378.

Widdel, F., Musat, F., Knittel, K., and Galushko, A. (2007) Anaerobic degradation of hydrocarbons with sulphate as electron acceptor. In *Sulphate-Reducing Bacteria: Environmental and Engineered Systems*. Barton, L.L., and Hamilton, W.A. (eds). Cambridge, UK. Cambridge University Press, pp. 265–303.

Wu, M., and Scott, A.J. (2012) Phylogenomic analysis of bacterial and archaeal sequences with AMPHORA2. *Bioinformatics* **28:** 1033–1034.

Yarza, P., Yilmaz, P., Pruesse, E., Glöckner, F.O., Ludwig, W., Schleifer, K., *et al.* (2014) Uniting the classification of cultured and uncultured bacteria and archaea using 16S rRNA gene sequences. *Nat Rev Microbiol* **12:** 635–645.

Yilmaz, P., Kottmann, R., Field, D., Knight, R., Cole, J.R., Amaral-Zettler, L., *et al.* (2011) Perspective minimum information about a marker gene sequence (MIMARKS) and minimum information about any (x) sequence (MIxS) specifications. *Nat Biotechnol* **29:** 415–420.

Yu, N.Y., Wagner, J.R., Laird, M.R., Melli, G., Rey, S., Lo, R., *et al.* (2010) PSORTb 3.0: improved protein subcellular localization prediction with refined localization subcategories and predictive capabilities for all prokaryotes. *Bioinformatics* **26:** 1608–1615.

Zhang, Z., Schwartz, S., Wagner, L., and Miller, W. (2000) A greedy algorithm for aligning DNA sequences. *J Comput Biol* **7:** 203–214.

Zhou, J., Bruns M.A.N.N., and Tiedje, J.M. (1996) DNA recovery from soils of diverse composition. *Appl Environ Microbiol* **62:** 316–322.

Zverlov, V., Klein, M., Lücker, S., Friedrich, W., Kellermann, J., Stahl, D.A., *et al.* (2005) Lateral gene transfer of dissimilatory (bi) sulfite reductase revisited. *J Bacteriol* **187:** 2203–2208.

Supporting information

Additional Supporting Information may be found in the online version of this article at the publisher's web-site:

Fig. S1. Evolution of sulfide (white symbols), sulfate (black symbols) and cell numbers (bars) in triplicate *Ca.* D. auxilii cultures grown with hydrogen and sulfate. Total cell numbers were determined by DAPI stained cell counts, fractions of *Ca.* D. auxilii and the contaminating archaeal cells were determined after dual CARD-FISH treatment with the *Ca.* D. auxilii specific probe (HotSeep-1_1465) and a general *Archaea*-targeting probe (Arch915). During the exponential growth phase 90 to 95% of all cells were identified as *Ca.* D. auxilii (grey bar area). The contaminating species (patterned bar area) was identified as *Archaeoglobus* sp. Note: The inoculum (t0) contained 80% *Ca.* D. auxilii and 20% archaeal cells; at t7 the culture contained 10% *Ca.* D. auxilii and 90% archaeal cells.

Fig. S2. Temperature dependency of sulfate reduction in *Ca.* D. auxilii cultures. Sulfate reduction rates were calculated from sulfide production observed in triplicate cultures over 3 weeks of incubation at the designated temperature.

Fig. S3. Effect of organic electron donors on the *Ca.* D. auxilii culture. Control incubations contained H_2 as electron donor (H_2 control) or no added electron donor (none). CO_2 was present as carbon source in all incubations. Grey squares: Sulfide concentration in replicate incubations per substrate after 21 days of incubation. Circles: Numbers of *Ca.* D. auxilii (green) and archaeal (red) cells per ml culture determined after 21 days of incubation in replicate incubations by CARD-FISH stained cell counts (probe HotSeep-1_1456 and Arch915). Cross: no cells detected. Incubations were performed at 60°C, medium was buffered with 30 mM bicarbonate, pH of medium (7.2) was altered <0.2 pH units upon substrate addition.

Fig. S4. Development of sulfide production by *Ca.* D. auxilii cultures incubated with different hydrocarbons (methane, propane, butane) compared to control incubations with hydrogen (circles) and without electron donor (diamonds).

Incubations were performed in duplicates (filled and open symbols). Sulfide production in hydrocarbon amended cultures was similar to the control without electron donor over 3 months. Incubations supplemented with hydrogen showed high sulfide concentrations after approximately 3 weeks proving that the culture used as inoculum was active.

Fig. S5. Effect of organic carbon sources on the *Ca*. D. auxilii culture. Hydrogen was present as electron donor in all incubations. Control incubations contained only CO_2 as carbon source while all other incubations contained CO_2 as additional carbon source (medium is bicarbonate buffered). Squares: Sulfate-reducing activity in replicate incubations per substrate tested (experiment was repeated twice: white squares incubation series 1; grey squares incubation series 2). Circles: Numbers of *Ca*. D. auxilii (green) and archaeal (red) cells per ml culture determined after 17 days of incubation in replicates from incubation series 2 (grey squares) by CARD-FISH stained cell counts (probe HotSeep-1_1456 and Arch915). Dashed line indicates median sulfate-reducing activity (grey) or median cell numbers per ml culture (green) of replicate control incubations (CO_2 plus H_2). Incubations were performed at 60°C, medium was buffered with 30 mM bicarbonate, pH of medium (7.2) was altered $<$0.2 pH units upon substrate addition.

Fig. S6. Correlation of sulfate reduction and carbon fixation in triplicate cultures of *Ca*. D. auxilii. Sulfate consumption (black symbols) and sulfide production (white symbols) in *Ca*. D. auxilii cultures grown with sulfate and hydrogen (circles) and in control incubations without electron donor (triangles) and abiotic control (squares). CO_2 fixation (bars) was determined by ^{14}C-bicarbonate uptake into particulate organic material. CO_2 fixation in control experiments (without electron donor and in abiotic control) is not visible. Sulfide development was determined in parallel incubations without ^{14}C labelling. During the exponential growth phase CO_2 fixation accounts for 2.4 to 4.1% of the sulfate reduction rate (3% on average).

Fig. S7. Effect of alternative sulfur compounds on activity of *Ca*. D. auxilii cultures.

A. Sulfide production by the *Ca*. D. auxilii enrichment in the presence of alternative sulfur compounds as sole energy source (open circles), with hydrogen as additional energy source (dark grey circles) and with hydrogen plus sulfate as additional energy source and electron acceptor (light grey circles). Sulfide concentrations determined after 17 days of incubation at 60°C. Sulfide production is only measured with sulfur and sulfate as electron acceptors in the presence of hydrogen.

B. Activity of the *Ca*. D. auxilii enrichment on hydrogen plus sulfur or sulfate as electron acceptors. Activity (calculated as reducing equivalents consumed to account for the different oxidation states of the sulfur compounds) is on average 10 times higher on sulfate than on sulfur. The enrichment on hydrogen plus sulfur could not be sustained in several attempts; hence observed minor sulfur reduction did not seem to support growth of *Ca*. D. auxilii.

Fig. S8. 16S rRNA gene based phylogenetic classification of *Ca*. D. auxilii and representative related sequences calculated applying the maximum likelihood algorithm (RAxML) with a 50% base frequency filter and 1000 replicates to estimate branch support. The phylogenetic position of the 16S rRNA gene of *Ca*. D. auxilii was not stable as indicated by a comparison of trees calculated by different methods (RAxML, PhyML and neighbor-joining; data not shown). Sequences in the *Ca*. D. auxilii cluster share $>$97.5% sequence similarity and affiliate with environmental sequences currently exclusively retrieved from the Guaymas Basin. Indicated are the accession numbers and the source of the sequence, for more details on these and other HotSeep-1 related sequences see Supplementary Table S1. Colour coding: black, genomic 16S rRNA of *Ca*. D. auxilii; red, obtained from Guaymas Basin enrichments on methane (Holler *et al*., 2011 Kellermann *et al*., 2012; Wegener *et al*., 2015); blue, obtained from Guaymas Basin enrichment on butane (Kniemeyer *et al*., 2007); green, obtained from Guaymas Basin sediments (Teske *et al*., 2002; Dowell *et al*., 2016).

Fig. S9. Phylogenetic classification based on the 23S rRNA gene. The phylogenetic tree was calculated with the RAxML algorithm and application of a 50% variability filter to exclude highly variable alignment regions. It is shown that the genomic 23S rRNA gene of *Ca*. D. auxilii affiliated with known syntrophically growing organisms of the class *Deltaproteobacteria*.

Fig. S10. Phylogenetic classification of the dissimilatory sulfite reductase gene, subunit A (*dsr*A) of *Ca*. D. auxilii. The phylogenetic tree was calculated from the amino acid sequence alignment of 256 sequences applying the maximum likelihood algorithm (RAxML) with the LG substitution model and employing a 30% variability filter to exclude highly variable alignment regions. Branch support was calculated from 100 replicates. The genomic *dsr*A of *Ca*. D. auxilii clusters with sequences from Guaymas Basin AOM enrichments incubated at 50°C and 60°C (red) and sequences from early hydrogenotrophic growing HotSeep-1 enrichments (blue) with $>$95% amino acid sequence similarity. The *Ca*. D. auxilii DsrA cluster affiliates with environmental sequences obtained from methane-rich estuary sediments (Baker *et al*., 2015) and relates to the DsrA sequences of *Desulfatiglans anilini* (formerly *Desulfobacterium anilini*), *Moorella thermoacetica* and *Desulfotomaculum* spp.

Fig. S11. A. Gene cluster encoding proteins potentially involved in electron transfer processes: formate dehydrogenase subunit B (*fdh*B), methyl-viologen-reducing hydrogenase subunit D (*mvh*D), electron transfer flavoprotein subunit A and B (*etf*A and *etf*B), heterodisulfide reductase subunit A (*hdr*A), FeS oxidoreductase (FeS OR). The FeS oxidoreductase encoded by HS1_002398 is an integral membrane protein while all other genes likely encode cytoplasmic proteins (inferred from TMHMM scan and PSORTb analysis).

B. Domain structure of the FeS oxidoreductase (HS1_002398) and comparison to the heterodisulfide reductase F (HdrF; WP_015905382 (HdrF3); Strittmatter *et al*., 2009) of *Desulfobacterium autotrophicum* HMR2 (domain structure determined with Interproscan and NCBI conserved domain search). HS1_002398 contains domains found in heterodisulfide reductases and six transmembrane helices, a domain composition previously described for HdrF of *D. autotrophicum* (Strittmatter *et al*., 2009). In contrast to the HdrF of *D. autotrophicum* HS1_002398 also encodes a multi-heme cytochrome c. The detected multi-heme (4 CXXCH motifs) cytochrome domain

overlaps with a predicted non-cytoplasmic region indicating that it may involve in periplasmic electron transfer reactions (see also Fig. 4). A similar HdrF-cytochrome fusion protein was not observed in a blastp comparison of HS1_002398 to the NCBI-nr database (highest identity 44%; maximal alignment coverage 84%, lacking the cytochrome c region). In the *Ca*. D. auxilii genome HS1_002498 is followed by genes encoding *etf*A and *etf*B (see A.), a clustering that is also observed for the *hdr*F3 gene of *D. autotrophicum*.

Table S1. Overview of available 16S rRNA gene sequences (nearly full length) related to *Ca*. D. auxilii with their isolation source, sequence similarity to the genomic 16S rRNA gene of *Ca*. D. auxilii and relative abundance of related sequences in thermophilic AOM enrichments (GB50 and GB60). Sequences >99% similar are marked by black lines and relative abundance of clones is given for each cluster observed in the thermophilic AOM enrichments. Grey shaded accession numbers are considered the closest related environmental sequences but are not classified as *Ca*. D. auxilii (based on a 97% sequence similarity threshold).

Table S2. Overview of single copy marker genes identified in the *Ca*. D. auxilii genome and their assigned phylotypes on phylum and order level. Single copy genes were identified from a set of 31 universal bacterial marker genes and phylogenetically classified using the AMPHORA2 software package (Wu and Scott, 2012). Marker genes in bold were used for phylogenetic reconstruction (see Fig. 3).

Table S3. Distribution of best scoring database hits of *Ca*. D. auxilii proteins across phyla and species.

Table S4. Reciprocal best match analysis of the *Ca*. D. auxilii genome versus genomes of selected organisms.

Table S5. Top scoring hits from blastn search of the genomic *Ca*. D. auxilii 16S rRNA gene sequence (1560 bp) against the NCBI database of 16S ribosomal RNA (*Archaea* and *Bacteria*); 17762 database entries, 13.10.2015.

Table S6. Classification of *Ca*. D. auxilii genes according to COG categories.

Table S7. Cytochrome c and pili genes of *Ca*. D. auxilii expressed during AOM (data taken from Wegener *et al*., 2015; Extented Data Table 4) and their corresponding locus tag in the *Ca*. D. auxilii genome (CP013015). For details see Wegener *et al*., 2015.

Table S8. Overview of HotSeep-1 ORFs used in Wegener *et al*., 2015 (Supporting Information Table 3a, b, 4a, b) and their corresponding locus tag in the *Ca*. D. auxilii genome (CP013015).